

WESTERN WASHINGTON UNIVERSITY

Bellingham, Washington 98225 • [206] 676-3000

April 25, 1983

Dr. Norm Gelfand, Chairman
Physics Advisory Committee
Fermi National Accelerator Laboratory
Batavia, IL

Dear Norm,

With this letter we are submitting 35 copies of the proposal "BATISS-Study of High Energy Neutrinos with a Deep Underwater Detector of a Mass Greater than 10^6 Tons." We hope the laboratory will look with kind eyes upon this rather unique and, as many say, imaginative experiment. We believe the laboratory, American science and, indeed, the world will benefit in the long run from this joint US-USSR international experiment. It is a "fixed target" neutrino experiment which Fermilab has a natural and unique advantage over all other accelerators in terms of beam energy and intensity.

A few of the unique scientific and technological benefits are listed in the preface of the proposal. For example, a quantum jump (two orders of magnitude improvement) can be expected in establishing new limits on oscillation lengths both momentum, and momentum independent. Perhaps there exists to be discovered, an oscillation length and a mixing angle which will fall within the range of sensitivity of the detector. The experiment may observe new and interesting properties of the beam. For example, the feasibility studies already carried out strongly suggest the existence of new neutrino-like particles. The next stage of the feasibility study will further elucidate the nature of these events.

There is also the series of neutrino beam applications which makes this experiment especially attractive to the general public. For example, we are pleased that our early idea on the use of neutrino beams for resource exploration is finding endorsement by notable scientists such as R.R. Wilson, Sheldon Glashow and others. We believe that BATISS is one truly unique experiment which has the features of extraordinarily high payout both scientifically and technologically. The costs will be derived from a special appropriations without hurting the regular high energy physics budget. We believe Leon Ledderman will find this a most worthwhile experiment also.

Co-spokesmen to this experiment are Seth Neddermeyer of the University of Washington (206-362-6437), Peter Kotzer of Western Washington University (206-671-4585), E.V. Kolomeets of Kazakh' State University, Alma-Ata and V.S. Murzin of Moscow State University.

Your careful considerations of this proposal will be appreciated.

Sincerely,

Peter Kotzer

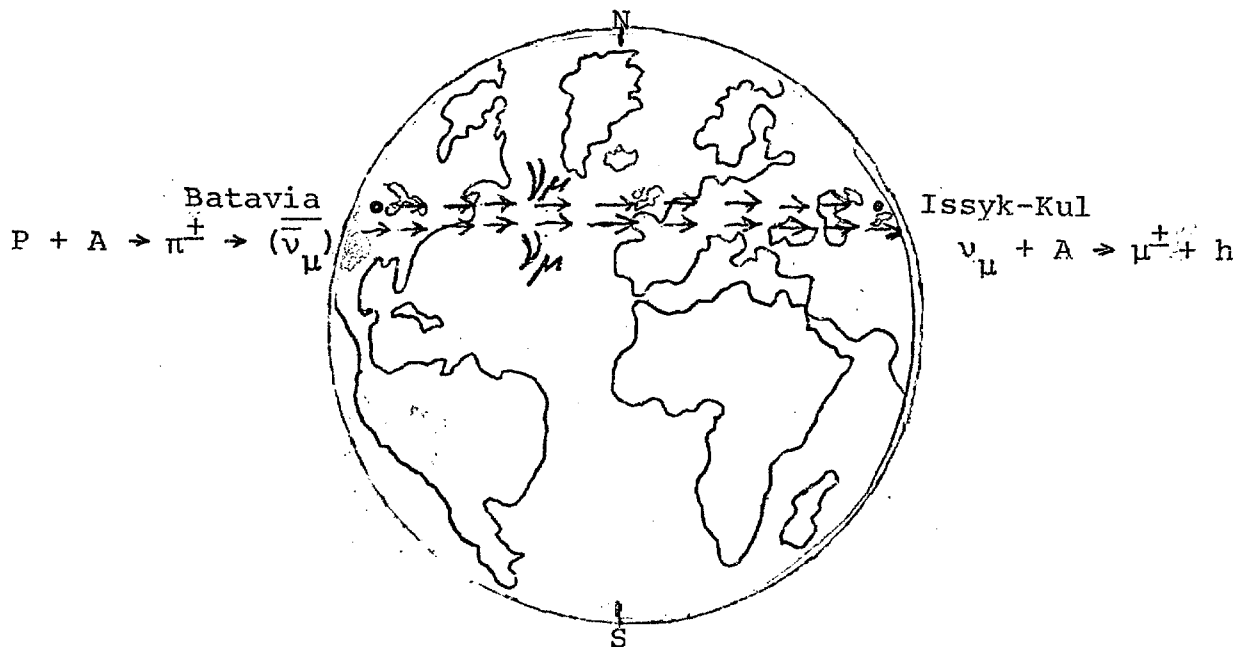
V. Murzin

Peter Kotzer and Vladimir Murzin

116 pgs.

EXPERIMENT BATISS

STUDY OF HIGH ENERGY NEUTRINOS
WITH A DEEP UNDERWATER DETECTOR
OF A MASS GREATER THAN 10^6 TONS



Peter Kotzer, Western Washington University
P.O. Box 5054, Bellingham, WA 98227

April 1983 Edition

BATISS - A Proposal for a Long Path Neutrino Experiment

By

P. Kotzer, J. Albers, R. Lord, A. Rupaal, R. Lindsay,
Western Washington University, Bellingham, Washington, USA

E.V. Kolomeets, L.A. Kostukevich, Iu.B. Prilepsky
Kazakh State University, Alma-Ata, Kazakhstan, USSR

V.S. Murzin, L.I. Saricheva
Moscow State University, Moscow, USSR

C.O. Alley,
University of Maryland

S.H. Neddermeyer, R. Davisson
University of Washington, Seattle, Washington, USA

S.N. Anderson, T.A. Koss
North Seattle Community College, Seattle, Washington, USA

Peter Kotzer: Spokesman

Western Washington University
Bellingham, Washington 98227

First Edition - March 1981
Second Edition - December 1981
Third Edition - January 1982
Fourth Edition - April 1983

ABSTRACT

We propose to study the properties of a 400 GeV wide band neutrino beam in a six million ton underwater Cherenkov light detector located in Lake Issyk-Kul 9,730 km chord line distance from Fermilab. This experiment can reduce the upper limit on the mass of tau neutrinos from 200 MeV to about 1 MeV. A large number of events will allow a significant improvement on the Δm^2 and the mixing angle in the momentum dependent oscillation length. The calorimetric and "fine" grain properties of the BATISS-BRISK detector will allow one to study the physics of neutrino-like events observed in the Western Washington University BATISS neutrino telescope detector. The paper, accepted for publication in the Proceedings of the 18th I.C.R.C. in Bangalore, India 1983 is attached. The proposed experiment is described in substantial detail in a booklet titled "Experiment BATISS - Detection of Muons and Neutrino Deep Underwater using a Detector with a Mass Greater than 10^6 Tons" - Western Washington University 1983.

Requests of Fermilab

1. One month of dedicated beam time be granted for the experiment. Funding support from sources other than high energy physics will provide for the cost of operations in the amount of 2 million dollars/month. The beam run would be generated at a time when Fermilab would be closed down because of a lack of operations funds.
2. It is requested that Fermilab bend the 400 GeV beam 45° below the horizon and point it toward the BATISS-BRISK detector.
3. That a total number of 2×10^{19} protons with an energy of 400 GeV be delivered to the neutrino detector.

Tata Inst Bangalore India 1983

SEARCH FOR NEUTRINO LIKE EVENTS 2750 KM FROM THE SOURCE

J.R. Albers, B. Faber, P. Kotzer, R.H. Lindsay, R. Lord, A. Rupaal
C. Schmidling, R. Webster; Western Washington University; S. H.
Neddermeyer, University of Washington; E. V. Kolomeets, Kazakh
State University; V. S. Murzin, Moscow State University.
P.O. Box 5054, Bellingham, WA, USA 98227

INTRODUCTION

This paper describes the results of a test for the existence of correlations between neutrino telescope events and the accelerator pulses produced by FNAL at 2750 km chord line distance. The neutrino telescope was aligned to select preferentially single particles coming up from 10 ± 6 degrees below the horizon. It could also detect particles, if any, which come from BNL at 3906 km chord line distance and 17 degrees below the local horizon. An atomic clock located at the FNAL measured the time of initiation of the Main Ring Ramp and the Main Ring Dump (which occurs after completion of the extracted 400 GeV beam), to a resolution of 10 μ s. The telescope records the time of occurrence of 4-fold coincidence events which are selected from a trigger on Cherenkov light signals produced by upward moving particles traveling along the axis of the telescope at the speed of light. A separate set of data which gives the index of the pulse, the intensity (of the Linac, Booster, Main Ring and fully accelerated beams), the time and date of production of each pulse and the cycle time is also discussed. Results of a search for correlation between the times of the observance of neutrino telescope events and the time of observance and the characteristics of the FNAL beam pulses will be given. Contributions of accelerator beams and beam losses in the form of background to cosmic-ray experiments will also be discussed.

DESCRIPTIVE

Preliminary to a full-scale experiment (BATISS) to study the processes involved in the penetration by a beam of high energy neutrinos through the earth at various chord lengths, this paper presents a partial analysis of some data obtained with a water Cherenkov counter telescope aimed at the FNAL from Western Washington University (WWU), Bellingham, along a 2750 km chord. Circumstances limit the present arrangement to viewing only those particles moving at rather large angles from the main beam line. Even if it had been possible to aim the telescope directly into the main accelerator beam the expected number of observable charged particles, arising from neutrino interactions in the intervening matter from FNAL to the telescope would have been impractically small with such a small effective target volume. Nevertheless, the experiment seemed to offer very interesting opportunities for the study of new processes and particles that have not yet been identified. Accordingly, the telescope was aimed 10 degrees below the horizon and in the azimuth of the accelerator. It was then necessary to use a

April 25, 1983

suitable event selection system capable of discriminating against a relatively huge cosmic-ray background and strongly favoring the selection of events containing one or more particles coming up from the earth.

The telescope consists of three cylindrical water tanks 1.2m in diameter by 1.8m long, mounted in tandem with photomultiplier tubes at the rear (upper) ends. Triggers on the simultaneous appearance of Cherenkov light signals in the front and back counters are called "AS" events because they are presumed to be identified mainly with the air showers of cosmic-rays. When the signal in the back counter lags by 26ns (the time of flight of a particle traveling at the speed of light up from the ground along the telescope axis) the coincidence is called a "TE" (telescope) event. About five months of telescope data have been recorded but only a small fraction has been analyzed, even partially. We deal here only with a 3 day run, May 24, 25 and 26, 1982, for which we had time synchronization data from Fermilab. The 3 day run recorded 194 TE events or 2.85 ± 0.11 per hour and 1546 AS events or 21.59 ± 0.30 per hour.

The AS event frequency is actually consistent with expected cosmic-ray flux and the TE events may likewise be largely produced by AS and by cosmic-rays that are scattered into the telescope from the earth. However, a small part of the TE events may have their ultimate source in the Fermilab whatever the intermediate processes may be. The first important problem is to establish various correlations that can contribute to this identification. Thus, the TE event rate may have a small positive correlation with the total power delivered by the Fermilab beam. A better test would be to relate the times as well as intensities of individual Fermilab pulses to the observed events.

In Figure 1 are plotted two 24 hour samples of the TE events, one from the 3 day run, and one from June 1 which had the two largest values, viz, 9 events per hour. Those two peaks are most probably only statistical fluctuations.

A computer program stepped through all of the pulses placing the time period between pulses into the beam-on category if the pulse preceding the telescope event had an extracted Main Ring (MR) beam, other wise it placed the time interval into the beam-off category. See Table 1.

Table 1 RESULTS

	N_{tot}	T_{min}	$\langle N_{tot} \rangle$	Excess	$N_p(MRinj)$
Beam-off	27	792	33.8	0	0
Beam-on	167	3738	159.9 ± 24	39	3.4×10^{17}
Total	194	4530	193.7		

A total of 27 beam-off TE in a 792 minute time period were observed compared to 167 in a 3738 minute beam-on time period. Two other analysis of two other sets of data show positive correlations. Hence, subtracting the background as determined by the beam-off rates from the number of events observed during the beam-on time period, an excess of 39 ± 24 "signal" events (1.6σ) is obtained. During this portion of the data run most of the 3.4×10^{17} Main Ring Injected protons were accelerated from 8GeV to 400GeV.

April 25, 1983

A further comparison between event rates observed during the active period (first 7sec) of the beam-on cycle time pulses and the dormant portion ($\Delta > 7\text{sec}$) of the beam-off portion of the cycle time suggests an excess of 14.8 ± 5.52 events or 2.4σ during the active stage. See Figure 2. A further comparison between the intensities of the data run average pulse of FNAL beams and the average intensity of the beam pulses immediately preceding and succeeding the observation of a neutrino telescope event shows that the "associated" beams are more intense by at least 2.0σ .

SUMMARY AND CONCLUSIONS

Three independent tests for the existence of correlations between neutrino telescope events 2750 km from FNAL and neutrino beam pulses yielded the following results.

1. Using the telescope 9 day average rate the beam-off rate was 2.8σ below expectation (while the beam-on rate was 0.61σ above expectation (from the null hypothesis). A minimum excess of 7 events was observed during the beam-on state. If the background to the beam-on portion of the data run was taken to be the beam-off rate then the excess of beam-on events is 46 with a deviation of 1.9σ . The probability that this excess is due to chance is .06.
2. If the beam-on and beam-off differences are real, then an excess of events should be observed during the active stages of the accelerator compared to the dormant stages. During this three day period the accelerator was cycling less than 13.5 seconds, less than 1% of the time. This included possible aborts. By defining the background rate to be given by the beam-off rates and by beam-on rates for $\Delta +$ values < 7.0 sec. we find that 66.2 ± 6.2 events are to be expected during the active stage, whereas we observe 81. The 14.80 excess of events during the active stages of the accelerator is 2.4σ above expectation. The probability that this excess is due to chance is 0.017.
3. If the excess events have their physical origin in the production of beam particles at FNAL, then the average intensity of beams associated with TE must be higher than the average taken over all pulses produced during the 3 day data run. The intensities of the Linac, Booster MR injection and MR accelerator components for the beam-on pulses are 2.5, 3.0, 3.0, 2.0σ above expectation respectively. However, the components of the beam-on and beam-off pulses are not independent. To be conservative, we take the intensity of the associated beams to be only 2σ above expectation. Hence, the probability that the higher intensity beams associated with the telescope events is due to chance is less than 0.05..

The combined probability that all three correlations independently are due to chance is $0.06 \times 0.017 \times 0.05 = (1/20,000)$. A minimum of 5 TE would have to be strategically shifted (a highly improbable occurrence) in a repeat experiment, to associated pulses with extremely low beam intensities in order to remove the excess. This improbable occurrence would remove the beam-off depletion and bring the intensity of associated beams to an average value. However, this would still leave an excess of at least about 10 events in the $\Delta +$ distribution (Figure 3). Hence, the analysis suggests that a minimum of 5 events/3 days are generated by some kind of beam particles from the FNAL, a distance of 2750 km from the source.

April 25, 1983

Acknowledgements

We thank C.O. Alley, S. Wagner, C. Steggerda, A. Khalil of the University of Maryland Quantum Electronics Group for providing the atomic clock for the Western Washington University neutrino telescope and the times of the initiation of the ramp and main ring dump of FNAL pulses. Further, we thank N. Gelfand, J. MacLaughlin, J. Crisp, H. Fenker and M. Storm of the FNAL for their assistance in supervising the atomic clock data and providing the data on the FNAL beam pulses. Valuable discussions with Robert Glasser and Richard Gustafson are gratefully acknowledged.

Reference: Experiment BATISS, WWU Ed. Bellingham, WA 1983.

April 25, 1983

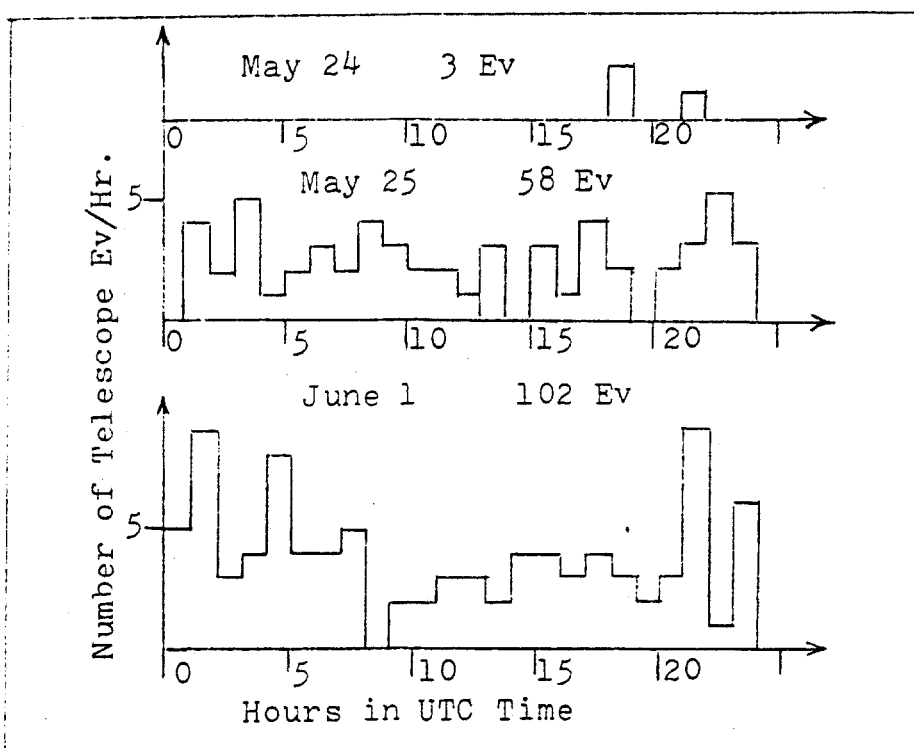


Figure 1 Hourly Arrival Rates of Neutrino Telescope Events

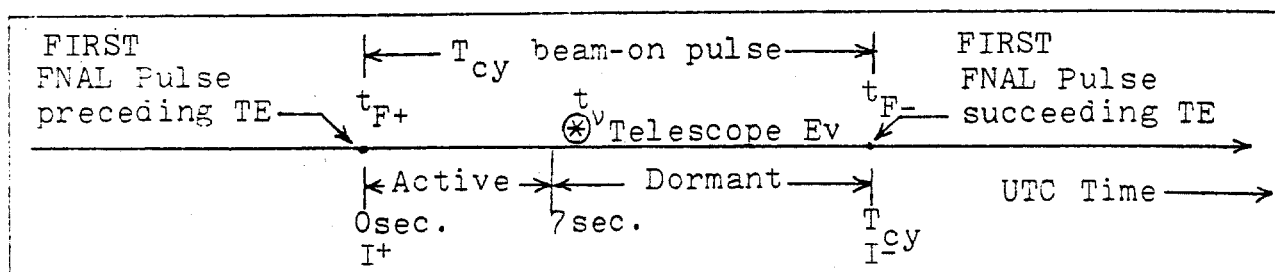
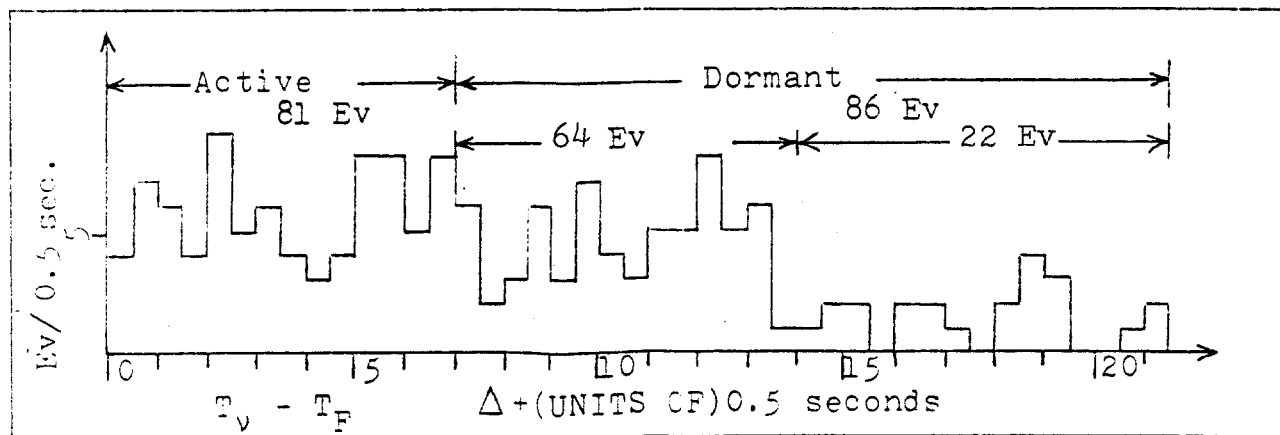


Figure 2 Definitions of Variables

Figure 3 Distribution of the $(T_v - T_F)$ of TE.

April 25, 1983

PREFACE

BATISS

BATISS is an acronym for BATavia where the high energy Fermilab accelerator is located and Lake ISSyk-Kul where a six megaton neutrino detector is to be located. In this experiment, very high energy neutrinos which are produced at the Fermilab are propagated through 9,370 km of earth to Lake Issyk-Kul where they will be detected and studied. The same detectors can be used for the study of high energy neutrinos of solar origin. This preface describes the basic elements and the structural framework of the BATISS experiment.

I. HISTORY

The idea of a joint U.S.-U.S.S.R. through-the-earth neutrino transmission experiment arose in a discussion at the International Conference on Cosmic-Rays in Plovdiv, Bulgaria in 1977 among U.S.S.R. scientists Professor E. V. Kolomeets of Kazakh State University, Professor V. S. Murzin of Moscow State University and U.S. scientists Professor Peter Kotzer of Western Washington University and Professor J. J. Lord of the University of Washington.

Since that time many theoretical calculations and technological studies in support of the experiment have been carried out. *These studies are strongly supportive of the feasibility of the BATISS experiment.*

II. AIMS OF THE EXPERIMENT

In the BATISS experiment the very high energy neutrinos which are generated by a very high energy accelerator such as that at the Fermi National Accelerator Laboratory in the U.S., and which travel 9,370 km through the earth to Lake Issyk-Kul will be detected and studied jointly by U.S.A. and U.S.S.R. scientists.

The results of the BATISS experiment will provide new and more precise answers to several classes of important problems.

First: Fundamental problems in high energy neutrino and elementary particle physics. Among these are:

- 1) The question of the stability of the ν_e, ν_μ, ν_τ neutrinos.
- 2) The question of the existence of oscillations of neutrinos amongst each other $\nu_e \rightleftharpoons \nu_\mu \rightleftharpoons \nu_\tau \rightleftharpoons \nu_e$.
- 3) The question of the existence of new earth-penetrating particles, i.e., neutral leptons.
- 4) The question of the existence of new interactions among known weakly interacting particles.
- 5) The question of the long term stability of the proton.

- 6) The question of the acceleration mechanisms in solar flares.

Second: Fundamental problems in the geophysical sciences. Major advances in this area are possible because measurement of global distances to an absolute error as small as a few millimeters may be possible. Thus BATISS will:

- 1) Provide new techniques for a global survey of the earth with unprecedented accuracy using neutrino beams. For this purpose the detector should be capable of observing neutrinos from several sources.
- 2) Provide a determination of the relative motion of two global points on different continents and possibly directly observe the predicted relative motion of tectonic plates.
- 3) Provide techniques and information for future experiments on the long term vertical motion of the ocean floor.
- 4) Determine directly the short term (diurnal) tidal motion of the earth which may be as much as 50 cm per day.
- 5) Correlate the possible changes in the motion of the plates with earthquake data.
- 6) With some modifications to the Issyk-Kul neutrino detector it may be possible to examine the theoretical prediction of the change of the gravitational constant with time.

Third: Applications. Upon the completion of the BATISS detector and analysis of neutrino events (and the answers to these fundamental problems in the sciences) several new applications of neutrino beams are possible.

- 1) An entirely new form of human communication. Techniques will be developed to demonstrate that neutrinos can be used to convey messages through the earth without the aid of electrical conductors.
- 2) Exploration for massive deposits of oil and minerals may be possible.

III. WHY A JOINT U.S.-U.S.S.R. EXPERIMENT

There are many advantages to a joint U.S.-U.S.S.R. BATISS experiment. Among them are:

1. The originators of the long base-line experiment, Drs. E. V. Kolomeets, V. S. Murzin, P. Kotzer, and J. Albers, will jointly direct the project. They are from the respective countries and have thought out the experiments in sufficient scientific and technological detail so as reasonably to anticipate the successful completion of the project.

2. Both countries have the necessary technological and scientific resources for carrying out the BATISS neutrino experiment
3. The source of the world's highest energy neutrinos already exists in the U.S. at the Fermilab. Since the ease of detection of neutrinos increases with their energy, it would be advantageous to use this source.
4. The source-to-detector distance, 9,370 km, is very large (almost as great as the earth's diameter), providing the opportunity for very sensitive tests of the existence of neutrino oscillations.
5. Lake Issyk-Kul, one of the world's largest bodies of clean water, is optimum for placement of a neutrino detector and the study of neutrinos. The Kazakh State University Laboratory can carry out the construction, deployment and operation of the underwater neutrino detector in collaboration with American scientists.
6. Valuable data on searches for and properties of neutrinos from the Fermilab can be taken soon after the detector is placed. After this study and search, bending of the proton beam can take place for further studies of the properties of neutrinos and also feasibility tests of transcontinental neutrino communications systems.

Already a working relation between scientists in the two countries exists. Prof. Kolomeets visited Western Washington University between January 8 and March 12, 1981 to work with the participants there to help solve the scientific and technological problems associated with the proposed experiment. Furthermore, an agreement between the respective institutions of the U.S.S.R. and the U.S.A. was signed on July 30, 1981 in Alma-Ata.

IV. PROGRESS ON THE BATISS EXPERIMENT

(1) In the U.S.S.R., measurements of water transparency, which were necessary to determine the number of detector elements, have been successfully carried out, proving that Lake Issyk-Kul will make an ideal location for an efficient detector of man-made and natural neutrinos.

(2) In the U.S.A. a working "mini" model of the BATISS detector, complete with the computer system, is in operation and has demonstrated that the detector can be constructed to achieve a sufficiently high resolution of the relative time of arrival of neutrinos between the modules in the neutrino telescope and that a global time synchronization system can be used to effectively cancel out the large background of cosmic-ray muon and neutrino noise events.

V. PROPOSED SCHEDULE OF FUTURE BATISS ACTIVITIES

In 1981:

(1) Conclusion of an official agreement should be achieved between the U.S.-U.S.S.R. participants as to the detailed division of tasks in the BATISS experiment. This is expected to occur during the December 15-January 15 meetings at Alma-Ata of this year.

(2) It will be necessary, in the interest of scientific advancement of BATISS, that a prototype neutrino telescope be operated by the U.S.S.R. The BATISS neutrino telescope should be emplaced and operated in Lake Issyk-Kul at a depth greater than 500 meters. It is necessary that the detector be a working portion, such as a section, neighborhood or possibly a ganglion of the full scale BATISS detector, and be as close in design as possible to the specially designed working telescope at WWU so as to eliminate possible discrepancies in the data attributable to instrument design.

(3) The successful operation of the neutrino detector requires that the condition of the beam of neutrinos at the Fermilab be correlated, on a real time basis, with the condition of operation of the BATISS telescope at WWU and the BATISS neutrino detector in Lake Issyk-Kul. It will be most beneficial to establish an "on line" communication link from the start of the BATISS experiment when background cosmic-ray muon and neutrino measurements are being carried out and the construction of the final BATISS Detector is in progress.

Timing will be based on the use of a system of synchronized atomic clocks located at the Fermilab and also at the Lake Issyk-Kul Neutrino Detector, or the use of an existing satellite.

In 1982:

(1) Measurement of the cosmic-ray muon and neutrino background in Lake Issyk-Kul. It will be desirable to carry out measurements of the background neutrinos from the Batavia, CERN and Serpukhov accelerators at this time. To do this, a large scale computer required for data analysis at Lake Issyk-Kul should be operational by the end of the year.

(2) Completion of a major portion of the BATISS Detector.

In 1983:

(1) Completion of the BATISS neutrino detector and initiation of a detailed study of the composition of the accelerator neutrino beam at wide angles.

(2) Searches for new neutrinos and studies of the Tau neutrino will be emphasized.

In 1984:

Operation of the BATISS neutrino detector in an intense Fermilab neutrino beam generated by one TeV energy protons.

VI. PUBLICATIONS

It is proposed that all publications be of joint U.S.-U.S.S.R. authorship and that the results derived from the activities related to the BATISS experiment be of joint ownership. The publications of the BATISS Neutrino Experiment results will be submitted simultaneously by the U.S.A.-U.S.S.R. authors to journals, in their respective languages.

VII. MEETINGS

Meetings between the scientists of both countries should be no less than two times a year. The times of the meetings should be chosen so as to optimize the progress of the BATISS experiment.

VEIII. EXCHANGES

The participants to be exchanged in the BATISS experiment will consist of both scientists and engineers but shall also include students from the participating universities or laboratories in both countries.

IX. CONCLUSIONS

The primary benefits of this joint experiment are: first, answers to questions of several fundamental problems in science and technology will be obtained, and, second, establishment of an improved working relation among the scientists of the U.S.A-U.S.S.R.

vii
CONTENTS

<u>Section</u>	<u>Page</u>
Preface.....	ii
Figures.....	xi
Tables.....	xii
Introduction	1
1.) Goals of the Experiment.....	3
2.) Advantages of the Proposed Experiment.....	4
3.) Physics Problems	
3.1) Oscillation of the Neutrino.....	5
3.2) Decay of the Neutrino.....	9
3.3) Neutrino Scattering-Angular Distribution.....	10
3.4) Heavy Charged Leptons.....	10
3.5) Unpredicted Phenomena.....	10
3.7) The Study of Anisotropy of Cosmic-Rays in an Energy Region Greater than 100 GeV.....	11
4.) Geophysical Problems.....	14
5.) Methods of Detecting High Energy Neutrinos.....	14
6.) Cross-Sections of Neutrino Interactions.....	15
7.) Accelerator Neutrinos.....	18
7.1) Production of Accelerator Neutrinos.....	18
7.2) Neutrino Beams from Accelerators.....	19
7.3) Transport of the Hadronic Beam and its Collimation.....	24

<u>Section</u>	<u>Page</u>
8.) Cosmic-Ray Neutrinos.....	25
8.1) Generation of Neutrinos by Solar Flares.....	25
9.) The Event Detection Rate.....	27
9.1) Geometry of the Accelerator Beam at the Detector.....	27
9.2) The Number of Interactions in the Detector from Accelerator Neutrinos.....	28
9.3) The Number of Interactions in the Detector from Solar Neutrinos.....	30
10.) Background.....	31
10.1) Muon Cosmic-Ray Background.....	31
10.2) Neutrino Background.....	32
10.3) Natural Radioactivity Background.....	33
11.) Synchronization of Detector and Neutrino Source Clocks.....	34
11.1) Synchronization Constraints for the Experiment.....	34
11.2) Mass of Heavy Neutrinos from Delays in Transit Time	35
12.) Cherenkov Light Detection.....	38
12.1) Transparency of Lake Issyk-Kul.....	38
12.2) Photomultiplier Sensitivity to Cherenkov Light.....	40
13.) The Detector.....	44
13.1) The Location of the Detector.....	44
13.2) The Modules.....	45
13.2.1) Soviet Version.....	45

<u>Section</u>	<u>Page</u>
13.2.2) The American Version.....	46
13.3) The Number of Modules in the Neutrino Detector.....	50
13.4) Geometry of the BATISS Detector.....	51
13.5) Calibration of Location of Modules.....	53
13.5.1) Geometrical Location of the Modules.....	54
13.5.2) Electronic Transit Time.....	54
13.5.3) Consistency Clocks.....	55
13.6) Detector Components.....	55
13.6.1) Programmable High Voltage Sources.....	55
13.6.2) Underwater Transmission Cables.....	56
13.6.2-1) Interfaces.....	56
13.6.2-2) Electrical Conductors.....	57
13.6.2-3) Optical Cables.....	57
13.6.2-4) Information Transmission Cables.....	58
13.6.2-5) Interconnection Cables Within a Section.....	58
13.6.2-6) Total Cable Length for the Array.....	58
13.6.3) The Electrical Power Requirements.....	59
14.) Data Generation and Analysis.....	60
14.1) Experiment Data Flow.....	60
14.1.1) Neutrino Source.....	60
14.1.2) Neutrino Detector.....	62
14.1.2-1) Cosmic-Ray Data.....	62

<u>Section</u>	<u>Page</u>
14.1.2-2) Accelerator-Neutrino Data.....	62
14.1.2-3) Array Monitor Data.....	63
14.1.3) Data Network.....	63
14.2) The Underwater Cherenkov Light Detector.....	64
14.2.1) Accelerator-Neutrino Detector.....	64
14.2.2) Cosmic-Ray Detector.....	64
14.3) Block Diagram of the Data Acquisition and Processing System.....	65
14.3.1) Module Structure.....	66
14.3.2) Module Grouping and Address Structure.....	68
14.3.2-1) Address.....	68
14.3.3) Trigger Hierarchy.....	71
14.3.3-1) Neighborhood.....	75
14.3.3-2) String Array.....	75
14.3.3-3) Gangleon.....	76
14.3.3-4) Transfer of Array Information...	77
14.4) The Detector Data Acquisition and Processing System.....	77
14.4.1) Preliminary Processing.....	78
15.) Budget Estimate.....	81
15.1) Estimates of the Materials Cost of the Mechanical Structure.....	81
15.2) Estimates of the Cost of the Electronics in the Data Acquisition System.....	82
15.3) Costs of Electronics for the Hexagonal Sections.....	84
15.4) Cost of On-Shore Data Processing Systems.....	85

<u>Section</u>	<u>Page</u>
16.) List of References.....	89
17.) Acknowledgments.....	92

FIGURES

1	Underwater Neutrino Cherenkov Light Detector Module - American Version.....	xiii
7-1	Energy Spectrum of Neutrinos from a 70 GEV Accelerator.....	20
7-2	Differential Spectrum of Neutrinos Interacting at FNAL Bubble Chamber.....	21
7-3	Angular Distribution of the Neutrino Flux at FNAL as a Function of Energy.....	22
7-4	FNAL Prompt Neutrino Fluxes.....	23
12.1	Schematic of Water Transparency Measurement/Module.....	41
12.1-2	Cherenkov Light and Kinematics.....	42
13.2-1	Schematic of a Spherical Module.....	47
13.2-2	Schematic of a Cylindrical Module.....	48
13.2-3	Schematic of a Two-Way Module.....	49
13.4	Schematic of a Section.....	52
14.1-1	BATISS Global Data Flow Diagram.....	61
14.3	Detector Data Acquisition Hierarchy.....	67
14.3.1	Module Electronics.....	69
14.3.2	Labeling of Modules in a Section, S_j	70
14.3.3	The Neighborhood N_h	72
14.3.4	Neighborhood Intelligence Center.....	73
14.5.1	SEL Version of the Detector Data Acquisition System.....	79

<u>Section</u>	<u>Page</u>
TABLES	
3.1	The Neutrino Oscillation Sensitivity
	Parameter for Some Neutrino Sources.....8
3.6-1	Proton Decay Modes.....12
3.6-2	Detection Efficiency.....13
10.1	Flux of Neutrinos from Cosmic-Rays.....32
14.3.3-1	Parts List for One Neighborhood.....75

INTRODUCTION

This proposal is published as the third in a series concerning long base line neutrino experiments and provides additional material on the overall plan for the implementation of the BATISS experiment. New technological advances in underwater neutrino detectors, time synchronization systems and high energy accelerator capability make possible transcontinental and truly international neutrino experiments.

This third edition is directed toward a more detailed layout of the proposed experiment--BATISS. We review specific physics and geophysics goals of the experiment and also bring up some applications of long base line neutrino experiments to geophysical and applied sciences. In later sections a specific design of both the underwater array and the data acquisition system is proposed along with estimates of costs for the associated materials.

A neutrino telescope, simulating the BATISS neutrino detector, is in operation at Western Washington University where problems of handling the cosmic-ray and electronic background and time synchronization techniques are being worked out. The Soviet Group is carrying out Monte Carlo studies regarding optimum array parameters and detection efficiencies of specific Cherenkov light module designs. The results of these studies will appear in other publications and will be summarized in another edition of the BATISS proposal.

The overall description of the BATISS experiment can best be understood in terms of three major technological problem areas which must be addressed by BATISS in order to insure a successful experiment. These are:

- 1) The production of a neutrino flux with known characteristics.
- 2) The construction and operation of a 10^6 ton or greater underwater neutrino detector.
- 3) The synchronization of times of neutrino beam generation with the times of recording of events at the BATISS detector.

The quality of the data and the degree to which the stated problems (physics and geophysics) can be worked out depends heavily on the technological framework of the experiment.

Sections 1-4 of this report describe the physics and geophysics problems addressed by this experiment.

Sections 5-6 methods of detecting neutrinos and their cross sections.

Sections 7-12 describe the properties of the neutrino sources (solar flares and accelerators), detection techniques and event rates.

Sections 13 and 14 give the design and layout of the experiment.

Section 15 gives an estimate for the cost of the detector.

1.) Goals of the Experiment.

The goal of the experiment BATISS (an acronym for BATavia - ISSyk-Kul) is the experimental study of the nature of neutrinos traversing large distances (on the order of $10^4 - 10^8$ kilometers) and large quantities of matter ($> 3.2 \times 10^9 \text{ g/cm}^2$). When the source of the neutrinos is an accelerator (in the present case, the Fermilab accelerator at Batavia), the experimental study is conducted with a neutrino beam with a strictly controlled intensity, energy, time of delivery and direction.

When the source of high energy neutrinos is solar flares, the distance from the source to the detector is also known, as is the energy spectrum of solar neutrinos from a determination of the energy spectrum of protons generated during the solar flares [7-9]. Also known is the somewhat more complicated trajectory and distribution in the arrival times of the cosmic-rays in the interplanetary field.

The neutrino beam produced by the accelerator protons at Batavia, Illinois, will be directed towards a deep and transparent lake located in the USSR--Lake Issyk-Kul--where the neutrino interactions will be observed in a water target with an effective mass of about 6×10^6 tons. The products of the nuclear interaction of the neutrinos in the water will be detected by the measurement of the Cherenkov light they produce.

In addition to the detection of accelerator generated neutrinos, the data acquisition system will make it possible to detect cosmic-ray muons at high energies ($> 10 \text{ TeV}$) and also optical-radiation generated by other sources of Cherenkov light such as the decay products of nucleons.

2.) Detector Site Advantages:

We have carefully considered many possible sites for the neutrino detector such as the arctic, the antarctic, Puget Sound, sites at the Bahamas, the Pacific Ocean and even the Great Lakes. Considering the many variables which have to be taken into account, location of the Underwater Neutrino Detector in Lake Issyk-Kul seems best.

We now enumerate some of the factors taken into consideration for this choice.

2.1) Source to Detector Distance:

Ideally it would be desirable to find a location on the opposite side of the earth which would match the cosmic-ray atmospheric neutrino source distance. A site in the antarctic was considered but discarded because of a lack of a staging area and because it was in the ocean where bioluminescence would be an important background. At higher energies (10 to 100 GeV) the flux of accelerator neutrinos will exceed the cosmic-ray neutrino flux. Coupled with higher event rates the closer distances are expected to yield a better limit or measure of the oscillation length. Lake Issyk-Kul to accelerator distance is about $3/4$ of the earth's diameter (9,370 km) and is quite satisfactory from the maximization of the source to detector distance.

Relative to other "on-site" accelerator and neutrino reactor experiments the source to the Issyk-Kul detector distance is:

- a) About 6,000 times greater than for on-accelerator-site locations.
- b) About 10^8 times greater when BATISS looks for solar flare neutrinos.
- c) About 8,000 times greater when atmospheric cosmic-ray neutrino beams are used.
- d) About 10^{17} times greater if and when neutrinos from the galactic center are the source.

2.2) Neutrino Target Mass Detector:

Compared to the largest on-site neutrino target mass detectors the BATISS detector will be 4,000 times greater. The detector cost will be less than most of the large scale on-site accelerator neutrino detectors and will have sufficient resolution to do the proposed physics.

Current underground neutrino water target detectors can also be used in long base line neutrino experiments but would suffer from about a thousand fold reduction in the event rate. The DURAND project would approach our scale but is confronted with special problems peculiar to the oceans, such as bioluminescence and strong deep ocean currents which present special marine engineering problems. Once these are overcome the DURAND detector would enjoy higher event rates.

2.3) Environmental Factors:

Placement of the detector in an area where weather conditions are mild reduces the cost of field operations.

In principle it is possible to operate the detector in the Arctic Ice Fields, but as has been pointed out by Professor Bogorodsky, the Arctic ice is in continuous motion, discouraging the choice of such a location for the neutrino detector.

In August 1979 a second location, Lake Baikal, was considered. This variant would also have many disadvantages compared to Lake Issyk-Kul, viz., that in the winter the winds are very strong and, further, the ice is in motion, frequently breaking up throughout the winter. Only a few months during the summer are available for work.

The Issyk-Kul site enjoys favorable conditions of weather and geographic location. Lake Issyk-Kul does not freeze in winter and therefore it is possible to work year-round at the site. Also, the Issyk-Kul site is "below" the current neutrino beam line.

A shallow water site in Lake Michigan was also considered. Such a site may be useful as an intermediate location before full bending of the beam.

2.4) Wide Angle Neutrinos:

The first BATISS experiment will carry out a search for neutrinos emitted at an angle of about 53° from the axis of the existing $N\bar{\nu}$ beam line. The flux of neutrinos may be larger than anticipated at this angle since neutrinos from decaying pions and kaons from the higher generations in the hadronic cascade will have a large angular spread which gives rise to wide angle neutrino fluxes. One interesting property of neutrinos at wide angles from the $N\bar{\nu}$ axis is that the relative flux of tau neutrinos compared to beam line center may be several orders of magnitude higher (because of the higher transverse momentum of the parent D^0 and F^\pm mesons) and will provide a cleaner beam for a search for tau neutrino oscillations and decays.

2.5) Access:

The availability of railroads, highways, airfields and water ports to and from the proposed Issyk-Kul detector site allows for inexpensive and rapid transport of heavy equipment and supplies.

Adequate living quarters and laboratory accommodations are also available at the lake shore staging area. The city of Alma Ata, a high technology center is less than 70 miles away from the detector site and can easily support the development and fabrication tasks for implementation of the detector.

2.6) Water Clarity:

Finally, Lake Issyk-Kul meets the necessary physical requirements for the dimensions, the water clarity and depth required for the operation of a large scale neutrino target mass detector. The lake has large regions which are about 700 meters deep. It is about 100 miles long, 40 miles wide and is as clear as distilled water with absorption paths of Cherenkov light as long as 50 meters and 50 to 20 meters near to the surface.

3) Physics Problems:

The BATISS experiment is designed to carry out important physics and geophysics experiments and also provide basic data for new technologies as summarized in the preface. This section points out some interesting physics problems which can be addressed in a unique way by BATISS.

3.1) Oscillation of the Neutrino

Neutrino oscillations were first postulated by Bruno Pontecorvo around 1957 to explain the lack of nuclear reactor neutrino interactions in the early Raymond Davis, Jr. experiments. Since that time a second neutrino, the mu neutrino has been discovered and strong circumstantial evidence from the Martin Perl, et al. experiments at SLAC points to the existence of a third. Many mechanisms have been postulated which predict transformations of neutrinos amongst themselves. The paucity of solar neutrino events [15] in the Homestake Gold Mine solar neutrino detector coupled with the development of a new class of Grand Unification theories which favors neutrinos with masses has provided a powerful impetus for implementation of the BATISS experiment. Neutrinos mixing (or oscillation) would provide a natural and beautiful explanation to the long standing solar neutrino puzzle and would provide valuable data for further development of theoretical attempts at Grand Unification.

Theoretically, oscillations might arise when neutrinos associated with normal weak interactions can take part in a new class of weak interactions having nonconserved lepton number. Such mixing would provide a natural resolution to the long standing solar neutrino puzzle [15]. In these

theories the mass of the neutrino is not zero, and the state vectors $|\nu_e\rangle, |\nu_\mu\rangle$ are themselves a superposition of state vectors of neutrinos with non-zero masses. For the case of two flavors

$$|\nu_e\rangle = \alpha_1 |\nu_1\rangle + \beta_1 |\nu_2\rangle$$

$$|\nu_\mu\rangle = \alpha_2 |\nu_1\rangle + \beta_2 |\nu_2\rangle$$

where $|\nu_1\rangle$ and $|\nu_2\rangle$ are the eigenstates of the two massive neutrinos. The results for the mixing of three types of neutrinos has been worked out by V. Barger, et al. [29]. If, as a result of some kind of weak process, a ν_μ beam is generated with a well-defined initial state, then at great distances from the source such a beam might be composed of a coherent superposition of muon, electron, and tau neutrinos. The oscillations are depicted as follows:

$$\nu_\mu \rightleftharpoons \nu_e \quad \nu_\mu \rightleftharpoons \nu_\tau \quad \nu_e \rightleftharpoons \nu_\tau \quad \dots \dots \dots (1)$$

It is necessary to note the following:

- 1) The difference in the masses of the states ν_1, ν_2 and ν_3 might be comparable with the μ_e, ν_μ , and ν_τ masses.
- 2) The oscillations of neutrinos may be either maximum or less than maximum. The amplitude for oscillations in neutral kaon beams is found to be maximum.
- 3) Given an initial beam of only one type of neutrino, at a later time the beam will consist of as many as three types assuming the ν_τ exists, and more if others exist.

Presently, there are several theories [10] of neutrino oscillations which predict the transition rates, W , for oscillations between ν_e and ν_μ at a distance R between the source and the

neutrino detector:

$$W_{\nu_e, \nu_\mu}(R) = W_{\nu_\mu, \nu_e}(R) = \frac{1}{2} \sin^2 2\theta (1 - \cos 2\pi \frac{R}{L}) \dots (2)$$

where $L = \frac{4\pi\hbar Pc^2}{|m_1^2 - m_2^2|c^4}$ is the oscillation length, P is the

momentum, and θ = degree of mixing.

As follows from the theory, oscillations might be observed best when $L \leq R$. Let $M^2 = |m_1^2 - m_2^2|$ then

$$L = 4\pi\hbar c Pc/M^2 c^4 \dots (3a)$$

Putting in the numerical factors we have

$$L = 2.5 Pc(\text{MeV})/M^2 c^4 (\text{eV})^2 \dots (3b)$$

When $M^2 c^4 \approx 1(\text{eV})^2$ and neutrino momentum is equal to 1 MeV, 10 MeV, and 1 GeV, the oscillation length is equal to 2.5 m, 25 m, 2.5 km, respectively. From Equation (3b) it follows that the effect of oscillation might be easily observed if:

$$M^2 c^4 \geq \frac{Pc}{R} 2.5 \dots (4)$$

In experiments to search for neutrino oscillations it is desirable to minimize the momentum of the neutrinos P_{\min} , and maximize the distance between the source and detector R_{\max} . The characteristic sensitivity of experiments in search of oscillations is given in terms of the parameter [11]:

$$M_{\min}^2 \approx 2.5 \frac{P_{\min}}{R_{\max}} \dots (5)$$

The parameter M_{\min} for various neutrino sources is given in Table 3.1. This table shows that the sensitivity of the proposed experiment would be two or more magnitudes greater than the present experiments [12, 20].

Table 3.1
The Neutrino Oscillation Sensitivity Parameter
for some Neutrino Sources.

Source-Detector	P_{\min} (MeV)	R_{\max} (meters)	M_{\min}^2 (eV) ²
Batavia Issyk Kul	5×10^4	8×10^6	1×10^{-4}
Solar Flare Issyk Kul	2×10^{-1}	1.5×10^{11}	3×10^{-12}
Solar Flare Issyk Kul	10^3	1.5×10^{11}	2×10^{-8}

EXPERIMENTAL LIMITS [35]

Baksan Cosmic-Ray ν_{μ}	1.4×10^3	1.2×10^7	$\leq 6 \times 10^{-3}$
----------------------------------	-------------------	-------------------	-------------------------

One possible method for determining the existence of neutrino oscillations consists of comparing the average intensity of observed neutrinos of a given type with the intensities expected in the absence of oscillations. This comparison is facilitated in an experiment of this type where the source spectrum and the intensity is known.

3.2) Decay of the Neutrino.

There are now strong theoretical arguments that the neutrino is not an absolutely stable particle as was thought several years ago. On the experimental side, in 1980 a report appeared in the Soviet Union by V. A. Lybimov et al. on the experimental determination of the mass of the electron neutrino. From a measurement of the end point of the β decay spectrum of Tritium it was reported to be about 25 eV [12]. A similar result (20 eV) has also been obtained by Simpson for the same process [22]. Although these experiments demand further confirmation, nevertheless, if one allows the mass of a neutrino at rest to be greater than zero, then, for example, in addition to an oscillation the neutrino might decay in the following manner:

$$\nu_1 \rightarrow \nu_2 + \gamma \dots \dots \dots (6)$$

The probability of this decay [11], has been calculated from the fundamental theory of weak interactions with neutrino mixing, and is given by the equation:

$$\Gamma(\nu_1 \rightarrow \nu_2 + \gamma) = \frac{9}{16} \frac{G^2_{\alpha}}{128\pi^4} m_1^5 \sin^2\theta \cos^2\theta \left(\frac{m_{\mu}^2}{m_w^2} \right)^2 \dots \dots \dots (7)$$

Here m_{μ} and m_w = masses of the muon and the intermediate vector

boson respectively. Additional decay modes of massive neutrinos have been investigated by Kolb and Goldman [30].

3.3) Neutrino Scattering - Angular Distribution.

In the proposed experiment it will be possible to determine the angle of scattering of neutrinos from nucleons, and also to obtain information about the parameter

$$M^2 = |m_1^2 - m_2^2|$$

The neutrino scattering angle can be calculated from a knowledge of the neutrino energy and the measurement of the hadron shower axis. Further the detector can measure the average angle of particles from the hadronic shower and the charged-current component. See Figure 12.1-2 for a brief discussion of the kinematics.

3.4) Possible Observations of the Birth of Heavy-Charged-Leptons.

Because of oscillations, if a neutrino of a new type such as ν_τ is part of the weak current together with charged heavy leptons, and if the neutrino field is entirely mixed, then it may be possible to observe the interaction of heavy charged leptons using a technique suggested by [31] if high resolution of the shower axis can be obtained by the BATISS detector software.

3.5) Unpredicted Phenomena.

It is necessary to note that in new experiments, there have frequently been found new, unknown, and unpredicted phenomena.

3.17 The Study of Anisotropy of Cosmic-Rays in Regions of Energy Greater than 100 GeV.

Project BATISS will detect particles from both the upward and downward directions. Muons detected from below are generated by the charged-current interaction of accelerator, atmospheric and cosmic ν_μ with the water in the lake and the lake bottom. Muons from the upper hemisphere will be predominantly of cosmic-ray origin via one or more secondary processes. Monitoring the

current interactions of high energy neutrinos with nucleons are the inclusive reactions:

$$\nu_{\mu} + N \rightarrow h + \mu \quad (9a)$$

$$\nu_e + N \rightarrow h + e \quad (9b)$$

where h are hadrons.

The typical neutral-current interactions of high energy neutrinos with nucleons are:

$$\nu_{\mu} + N \rightarrow h + \nu_{\mu} \quad (10a)$$

$$\nu_e + N \rightarrow h + \nu_e \quad (10b)$$

As a result of reaction (9a), high energy muons are created, carrying away on the average about one-half the incident neutrinos' energy and the other half going into a creation of an electromagnetic-hadronic shower (EMHS).

These interactions may be detected by observing the Cherenkov radiation emitted by the newly created relativistic charged particles which arise from the initial interactions of the neutrinos and the secondary and higher generation processes in the transparent water. Lake, sea, or ocean water may be used as the neutrino target detector media. The ocean water has a very serious background, viz., bioluminescent light. Cherenkov radiation can be easily measured with the help of photomultipliers arranged in the water and reliably protected from background sources of light in the case of lake water (or deep mines).

6.) Cross Sections of Neutrino Interactions.

An important feature of the interactions given in Eq. (9) and Eq. (10) is that the neutrino-nucleon cross-sections increase with the energy of the incident neutrino in the interval of

energy from 1.5 GeV up to 150 GeV [13].

The charged-current cross-sections for the interactions of neutrinos with protons and neutrons can also be given in terms of the quark structure functions :

$$\frac{d^2\sigma}{dx dy} (\nu_\mu p \rightarrow \mu^- h) = \frac{G^2 2mE_\nu}{\pi} \left(d_p(x) + (1-y)^2 \bar{u}_p(x) \right) x \dots (11a)$$

$$\frac{d^2\sigma}{dx dy} (\nu_\mu n \rightarrow \mu^- h) = \frac{G^2 2mE_\nu}{\pi} \left(d_n(x) + (1-y)^2 \bar{u}_n(x) \right) x \dots (11b)$$

where:

$x = Q^2 / (2m(E_\nu - E_\mu))$ is the Bjorken scaling variable.

$y = (E_\nu - E_\mu) / E_\nu = E_h / E_\nu$ energy carried by the hadron.

$Q^2 = 2E_\nu E_\mu (1 - \cos \theta_{\nu\mu})$ negative of the 4-momentum transfer squared.

$d_p(x)$, $d_n(x)$ are the structure functions for the down quark in the proton and the neutron respectively.

$\bar{u}_p(x)$, $\bar{u}_n(x)$ are the structure functions of the anti-up quarks in the proton and the neutron respectively.

E_ν is the energy of the incident neutrino.

E_μ is the energy of the muon generated by the charged current interaction.

$\theta_{\nu\mu}$ is the angle between the vector momenta of the incident neutrino and the resultant muon.

G^2 is the Fermi coupling constant.

m is the mass of the nucleon.

At low 4-momentum transfer the quark composition of the proton and the neutron respectively is:

$$p = uud, n = ddu.$$

The cross sections for neutrinos and antineutrinos on protons for $E_\nu > 10$ GeV are:

$$\sigma(\nu_{\mu} p) = [0.714 \pm 0.036] \times 10^{-38} \text{ cm}^2 E_{\nu} \dots \dots \dots (12a)$$

$$\sigma(\bar{\nu}_{\mu} p) = [0.371 \pm .019] \times 10^{-38} \text{ cm}^2 E_{\nu} \dots \dots \dots (12b)$$

where σ is in units of cm^2 , and E_{ν} is in units of GeV [24].

The energy independent part of the cross section for the interaction of high energy neutrinos with protons is about twice as high for energies ($E_{\nu} > 10 \text{ GeV}$) as it is for lower energies ($E_{\nu} < 10 \text{ GeV}$).

More recently, an exposure of 15 m^3 (2.2 tons) of deuterium to a neutrino beam produced by 5×10^{18} protons of 350 GeV energy at the Fermilab [23] has shown that:

$$\sigma(\nu_{\mu} n)/\sigma(\nu_{\mu} p) = 2.03 \pm 0.28; E_{\nu} = 50 \text{ GEV} \dots \dots \dots (12c)$$

$$\sigma(\bar{\nu}_{\mu} n)/\sigma(\bar{\nu}_{\mu} p) = 0.51 \pm 0.16; E_{\nu} = 40 \text{ GEV} \dots \dots \dots (12d)$$

in agreement with the model of the quark composition of the nucleons.

Taking into account Equations (12a, 12c) we compute:

$$\sigma(\nu, Z, A) = (2A - Z)\sigma(\nu p) \dots \dots \dots (13)$$

Taking for example $A = 18$ (water) $Z = 10$ and considering a beam of neutrinos of energy $E_{\nu} = 50 \text{ GeV}$ (which is not the maximum produced by the accelerator) we get

$$\sigma_{\nu}(A = 18) = (26) \times 0.71 \times 10^{-38} \times 50 = 9.23 \times 10^{-36} \text{ cm}^2 \dots (14)$$

The mean free path, λ_{ν} , of neutrinos in water is given by:

$$\tau_{\nu} = \lambda_{\nu} \sigma = 9/(13N\sigma(\nu p))$$

where $N = 6 \times 10^{23}$ nucleons/gram of matter and τ_{ν} is the mean free path in gm/cm^2 . Thus:

$$\tau_{\nu} = \frac{1.6 \times 10^{14}}{E_{\nu} (\text{GeV})} \text{ gm/cm}^2 \dots \dots \dots (15)$$

Assuming that the ν cross section continues to rise linearly with the energy then the mean free path of neutrinos with an energy of 22 TeV in matter of density 5.52 grams/cm^3 is the diameter of the earth.

7.) Accelerator-Neutrinos.

7.1) Production of Accelerator-Neutrinos.

The beam of accelerator-neutrinos is formed from beams of pions and kaons, as a result of their decay.

$$\pi^\pm \rightarrow \mu^\pm + \nu_\mu (\bar{\nu}_\mu) \quad (16)$$

$$K^\pm \rightarrow \mu^\pm + \nu_\mu (\bar{\nu}_\mu) \quad (17)$$

The major fraction of the neutrino beam is composed of neutrinos which result from the two particle decay processes of Eqs. (16) and (17).

The dynamics of two particle decays are well known, and in particular the momentum of neutrinos in the center of mass coordinate system is:

$$\bar{P}_\nu = \bar{E}_\nu = \frac{M_o^2 - M_\mu^2}{2M_o} \quad (18)$$

where M_o is the rest mass of the pion or kaon. So, for reaction (16) $\bar{E}_\nu = 0.037 \text{ GeV}$ and for reaction (17) $\bar{E}_\nu = 0.233 \text{ GeV}$.

In the laboratory coordinate system, the momentum distribution of the decay products is given by:

$$\frac{1}{N} \frac{dN}{dE} = \frac{M_o}{2P_\nu \bar{P}_\nu} = \text{constant} \quad (19)$$

Where N , the number of neutrinos with momentum P_ν , is bounded by the limits:

$$\gamma_o(\bar{E}_\nu - \bar{P}_\nu) \leq E_\nu \leq \gamma_o(\bar{E}_\nu + \bar{P}_\nu) \quad (20)$$

and γ_0 is the center-of-mass Lorentz factor. Using Eq. (18),

$$0 \leq E_\nu \leq 2\gamma_0 \bar{P}_\nu = \gamma_0 \left(\frac{M_0^2 - M_\mu^2}{2M_0} \right) \dots \dots \dots (21)$$

assuming that the mass of the neutrino is zero.

The maximum energy and momentum of neutrinos are dependent on the energy of the parent particle:

$$(E_\nu^k)_{\max} = 0.95 E_K \dots \dots \dots (22a)$$

$$(E_\nu^\pi)_{\max} = 0.43 E_\pi \dots \dots \dots (22b)$$

The maximum flux of electron neutrinos is several percent of the total beam and occurs mostly in the channel:

$$K \rightarrow e + \pi + \nu_e \dots \dots \dots (23)$$

For initial energy spectra of pions or kaons $W(E_0)$ it is easy to find the energy spectra of neutrinos.

$$\frac{1}{N} \frac{dN}{dE_\nu} = F(E_\nu) = \frac{2M_0}{2\bar{P}_\nu} \int \frac{W(E_0)}{P_0} dE_0 \dots \dots \dots (24)$$

The energy spectra of neutrinos, generated in the above manner, for energies up to 20 GeV [1] are shown in Figure 7-1. For beams of neutrinos of energy greater than 20 GeV (such as are produced in the Fermilab [20]) the energy spectra are shown in Figures 7-3, reference [25], and 7-4, reference [26].

The break in the neutrino spectra is the result of contributions of neutrinos from the channel denoted by Equation (17).

The spectrum of neutrinos producing muons emerging out of a ground target is shown in Figure 7-2.

7.2) Neutrino Beams from Accelerators.

Neutrino beams are generated in the following stages:

- 1) Protons, accelerated in an accelerator, impact on a thin

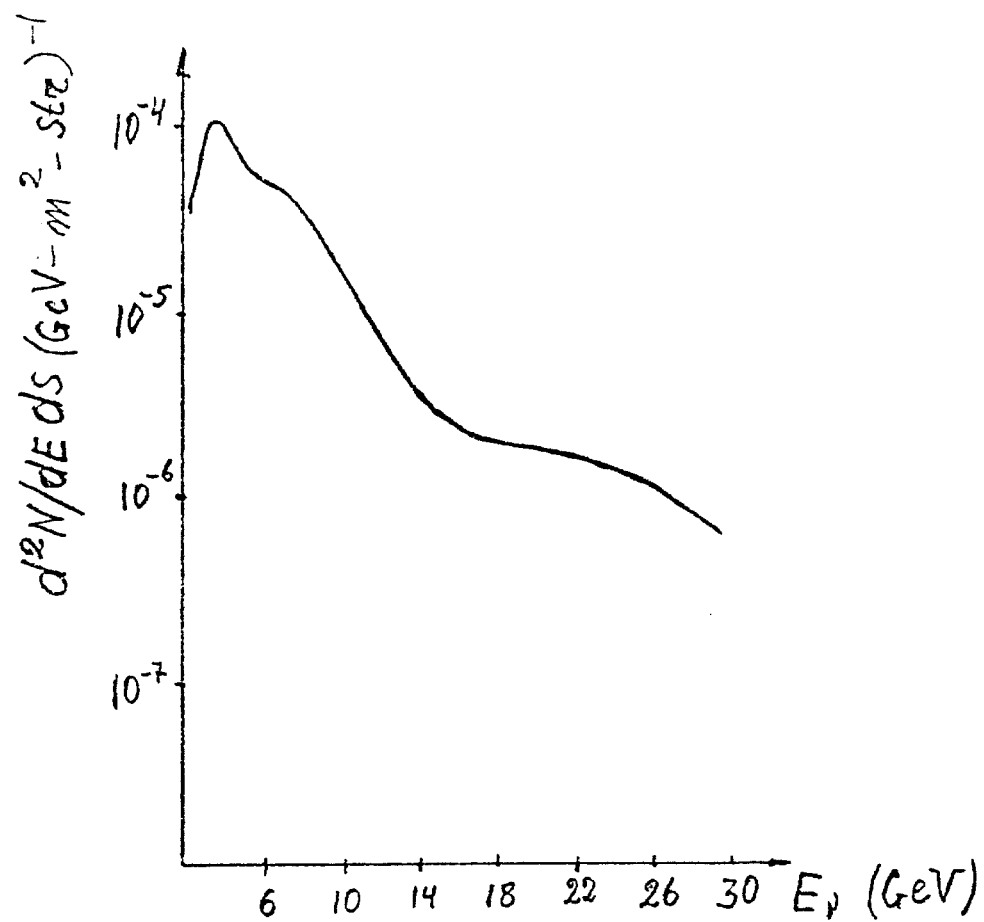


Figure 7-1 ENERGY SPECTRUM OF NEUTRINOS FROM A 70 GeV ACCELERATOR

Figure 7-2 Differential Spectrum of Interacting Fermilab Neutrinos Producing Muons Which Emerge From the Berm at the Bubble Chamber Site (1.4 km From the N-Ø Proton Beam Stopper). Based on the Fermilab Neutrino Flux by Malensek, Feb. 1979 (400 Meter Decay Tunnel, Two Horn Wide Band Focus).

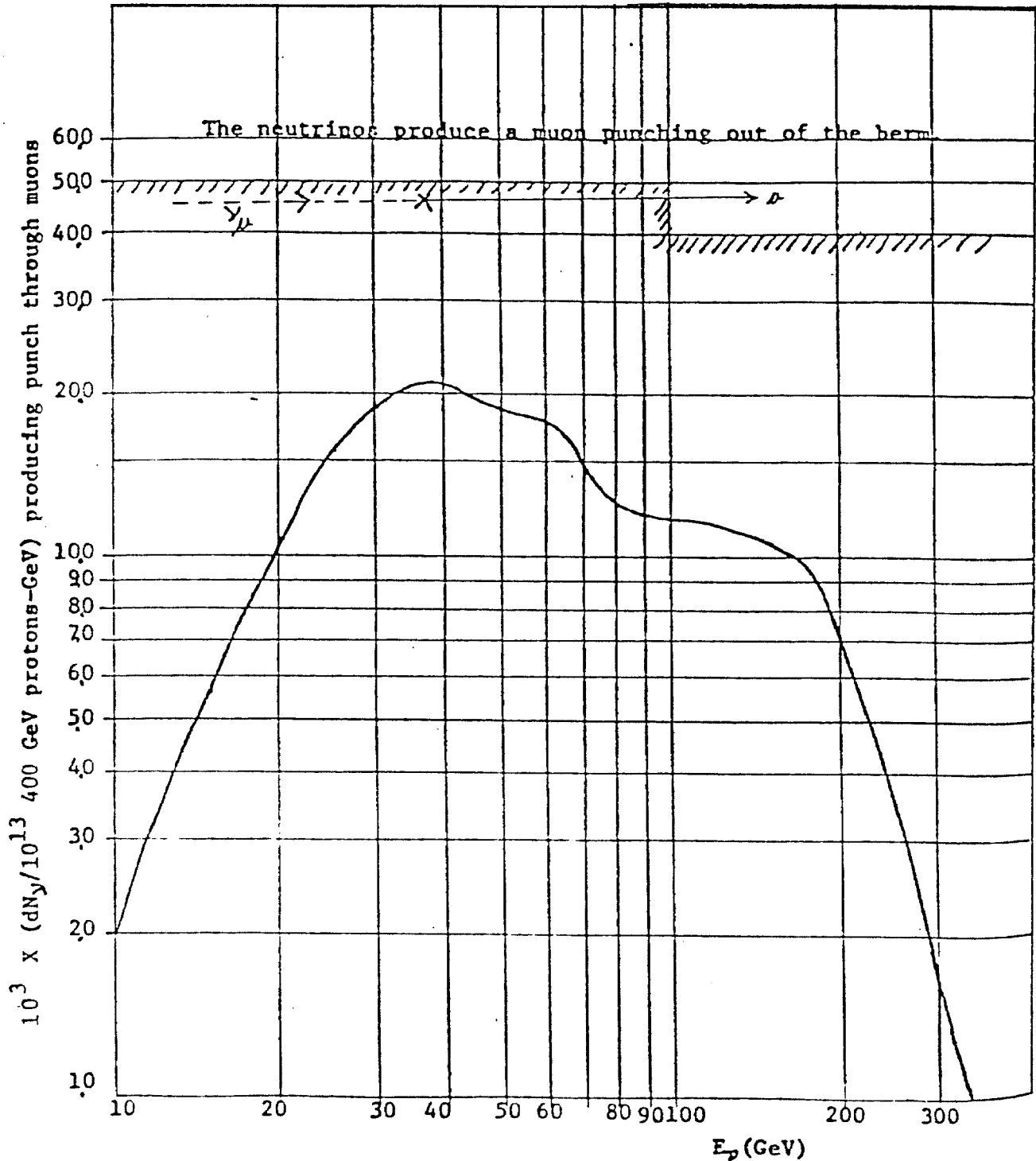


FIGURE 7-3

 ν Flux vs. Energy (Horn)

400 GeV Protons on Target

400 Meter Decay Pipe 1 km Shield

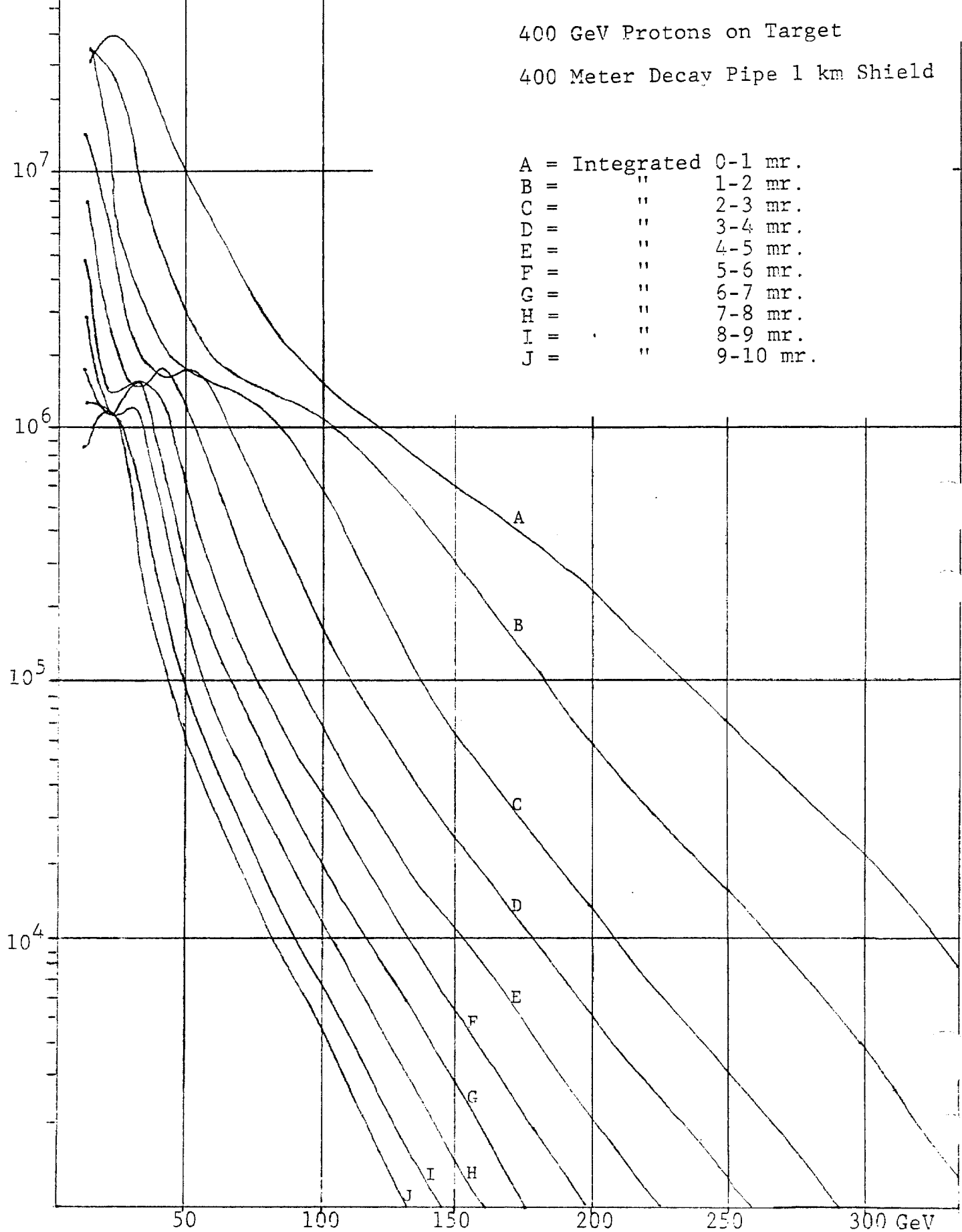
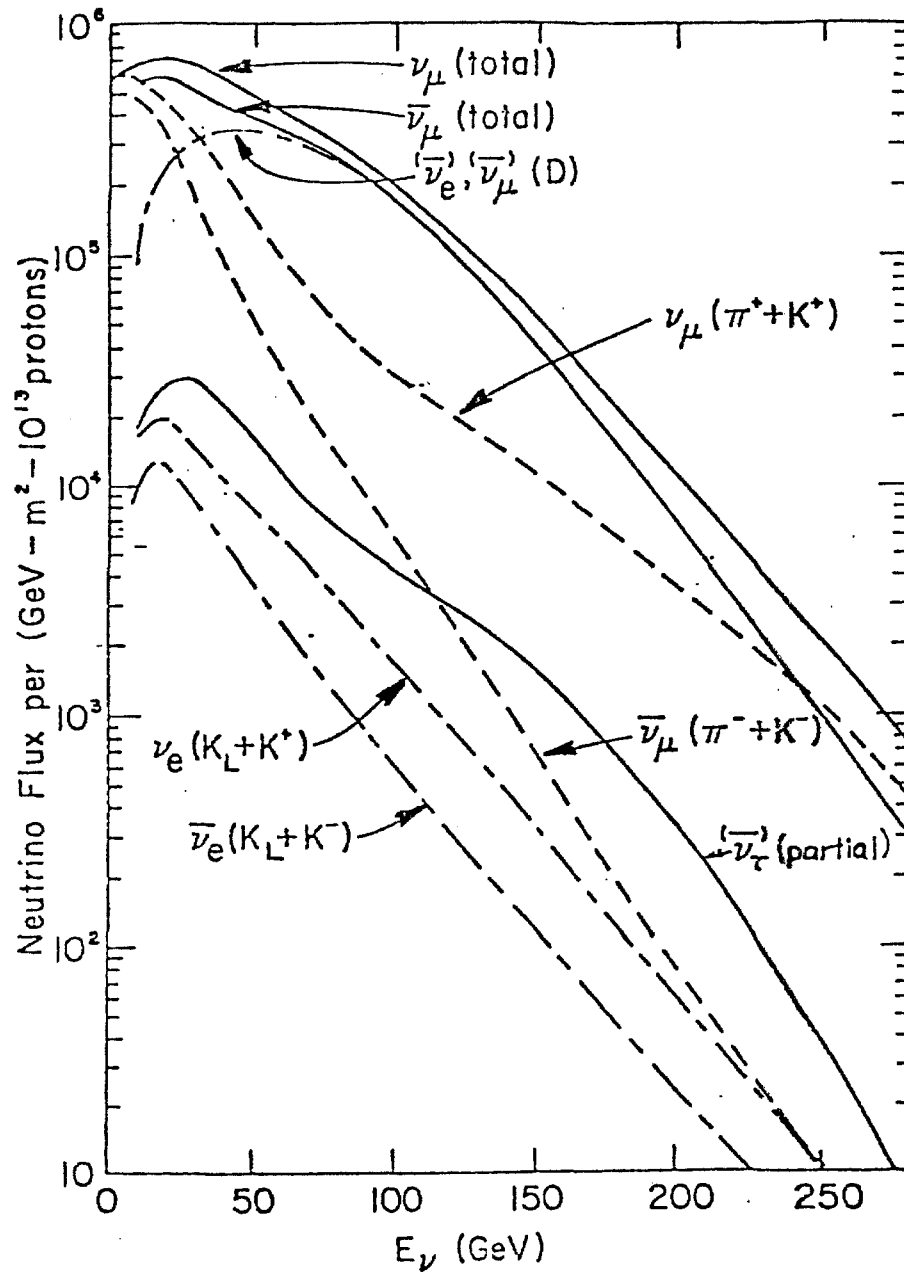
Flux/GeV/m²/10¹³ Incident Protons

Figure 7-4 Fermilab Prompt Neutrino Fluxes



target generating a secondary beam of hadrons.

2) These secondary hadrons are separated by signs of charge and by momentum with the help of a magnetic transport system.

3) Monochromatized secondary particles are fed into a decay tunnel (0.4 km in the case of the Fermilab NØ beam) where the reactions in Equations (16) and (17) take place, and the neutrino beams appear and propagate through the tunnel.

4) The mixed beam falls on a thick filter which absorbs the remaining hadrons and muons from decay reactions (16) and (17). At the accelerator, beams are created with a wide range of band widths. In the wide band beams focus is obtained with the help of "magnetic horns" which select particles of a like sign of charge.

Narrow band beams are formed from specially prepared chromaticized beams of hadrons and are subsequently focused. After the second focus and momentum selection, the beam has a narrow momentum spread $\Delta p/p \sim 0.05$ and a narrow angular divergence of 0.14 milliradians. The overall intensity of the narrow band is 100 times less than the wide band, but it is several times more effective due to better angular and energy characteristics.

The intensity of wide band beams in the interval of 2×10^{-3} radians consists of 10^{10} neutrinos at an average energy of about 50 GeV [14].

7.3) Transport of the Hadronic Beam and its Collimation.

A neutrino beam directed towards Lake Issyk-Kul will be obtained by bending a collimated beam of secondary hadrons which are transported and decay into neutrinos and other charged particles in a vacuum decay tunnel.

The length of the vacuum tunnel should be no less than one kilometer with a radius 15 - 20 centimeters. If there is no vacuum, the neutrino beam weakens by a factor of three because of degradation in energy by interactions of secondary particles with air nuclei in the decay tunnel.

8.) Cosmic-Ray Neutrinos.

8.1) Generation of Neutrinos by Solar Flares.

A detector with a mass greater than 10^6 tons allows the detection of muon neutrinos generated by intense solar flares. The neutrinos arise from the interactions of protons, accelerated to high energies in solar flares, with atomic nuclei near the solar surface. Detection of solar flare muon neutrinos makes it possible to search for neutrino oscillations with periods of several minutes, and also to study questions of the physics of the solar flares such as the time for acceleration of particles to high energies during flares; the time of their diffusion in the corona, and other questions.

As was noted by B. E. Pontecorvo (private communication), the magnitude of the flux of muon neutrinos from the sun is closely tied with the flux of other particles, charged and neutral, which in turn are easily observed in particle experiments. Taking into account that for muon neutrinos generated by the channel in Equation (16), the intensity is approximately equal to the intensity of photons generated in the reaction:

$$\pi^0 \rightarrow 2\gamma \quad (25)$$

We note two special classes of solar flare events, those from:

a) the generation of protons emitted from flares on the visible side of the solar disc.

b) the generation of protons from flares on the opposite side of the solar disc.

Case b) is more favorable for detection. The solar flare particles generated on the other side of the solar disc produce a sharper pulse of neutrinos. However, those which come to the earth from the visible side disperse in the interplanetary magnetic fields arriving in a wider time interval at the earth's atmosphere, thereby producing a wider and more diffuse beam of neutrinos, with a lower signal to noise ratio.

The number of neutrinos from flares on the opposite side of the sun will equal:

$$N_{\nu}(E_{\nu}) = N_p(E) \frac{N_{\pi}(E_{\pi})}{N_p(E)} \frac{N_{\nu}(E_{\nu})}{N_{\pi}(E_{\pi})} \dots \dots \dots (26)$$

where $N_p(E)$ = differential spectra of protons generated during solar flares [1]. N_{π} and N_{ν} are the number of pions and the number of muon neutrinos respectively.

The estimate of muon neutrinos is carried out by assuming an isotropic distribution of protons during flares and assuming that the energy spectra of the protons at the source can be written as:

$$N_p(E_o) = N_p^o A E_o^{-\gamma} \dots \dots \dots (27)$$

where N_p^o = total number of protons generated from a solar flare, E_o is the proton energy and γ is the spectral index. Let $f(E_{\pi}, E_o)$ be the probability of a proton of energy E_o producing a pion of energy E_{π} .

$$dN_{\pi}(E_{\pi}) = \int_{E_{\pi}}^{\infty} N_p(E_o) f(E_{\pi}, E_o) \left(\frac{dE_{\pi}}{E_o} \right) dE_o \dots \dots \dots (28)$$

Then :

$$\frac{N_{\pi}(E_{\pi})}{N_p^0} = \frac{AE_{\pi}^{-\gamma}}{1 + \gamma} \int u^{\gamma-1} f(u) du \dots \dots \dots (29)$$

$$u = E_{\pi}/E_o; \int f(u) du = N_{\pi} \dots \dots \dots (30)$$

$$(N_{\pi}/N_p) = N_p(E_{\pi}) N_p^0 A E_{\pi}^{-\gamma} = \langle N_{\pi} u^{\gamma-1} \rangle \approx 3 \times 10^{-2} (\gamma = 3) \dots \dots \dots (31)$$

An analogous calculation gives:

$$N_{\nu}(>0.5 \text{ GeV})/N_{\pi}(>0.5 \text{ GeV}) = (1/\gamma)(2E_{\nu}^*/M_{\pi})^{\gamma-1} \approx 6 \times 10^{-2} (\gamma=3) \dots (32)$$

and from (31) and (32):

$$N_{\nu}(>0.5 \text{ GeV}) \approx 2 \times 10^{-3} N_p^0(>0.5 \text{ GeV}) \dots \dots \dots (33)$$

In such a manner the integral flux of neutrinos with energies greater than 0.5 GeV generated during solar flares, will lie within the limits:

$$N_{\nu}(>0.5 \text{ GeV}) \approx (10^{25} + 10^{31})$$

corresponding to the integrated flux of protons for typical flares of:

$$N_p(>0.5 \text{ GeV}) \approx (10^{28} + 10^{34})$$

9.) The Event Detection Rate.

9.1) Geometry of the Neutrino Beam in the Locale of the Detector.

The sensitive volume of the detector is $180 \times 180 \times 180 \text{ m}^3$, where the height is 180 meters. The area of the detector is $A_d = 32,400 \text{ m}^2$, and its radius is $R_o \approx 100 \text{ m}$. Wide-band beams, having an angle of dispersion 2×10^{-3} radians, will appear as a circular spot of radius $R_{\max} \approx 2 \times 10^{-3} \times 9 \times 10^3 \text{ km} = 18 \text{ km}$ from the axis of the beam, so that the area of water illuminated by the beam is $A_{\nu} = 1018 \text{ km}^2$. The portion $\delta W = A_d/A_{\nu}$ intercepted by the detector is:

$$\delta W_w = 3.24 \times 10^{-2} \text{ km}^2 / 1018 \text{ km}^2 = 2.94 \times 10^{-5} \dots (34)$$

For narrow-band beams the portion intercepted will be greater because the angle of dispersion $\theta_n \approx 1.4 \times 10^{-4}$ radians is smaller. Thus $R_{\max} = 1.31 \text{ km}$.

$$\delta W_n = (3.24 \times 10^{-2} \text{ km}^2) / (5.41 \text{ km}^2) = 0.60 \times 10^{-2} \dots (35)$$

Thus, the fractional number of neutrinos in the narrow-band beam intercepted by the detector is about 200 times more than those intercepted from the wide-band beams. Since the total number of neutrinos in the wide-band beam is about 100 times more than the narrow-band beam, the number intercepted from the narrow band beam is about two times greater at the same average energy than from the wide band beam.

9.2) The Number of Interactions in the Detector from Accelerator Neutrinos.

Using the estimates given by Equations (34), (35) and the result in equation (15) it is possible to find the number of interactions in the detector with the area stated in Section 9.1.

For each calculation there are two variants of the neutrino detector geometry and two variants of the beam. As an example we discuss the case when the height of the detector, h , is 30 meters with a wide-band beam. The probability, P_i , of a neutrino interacting within the array is given by $P_i = h/\tau_\nu$ where τ_ν , the neutrino interaction mean-free path is given by Equation (15). Then the number of muons per pulse from (50 GeV) neutrino interactions is given by:

$$\begin{aligned} N_\mu &= (I_\nu)_w^0 \delta W_w (3.10^3 \text{ gr/cm}^2) / (3.2 \times 10^{12} \text{ grams/cm}^2) \\ &= (I_\nu)_w^0 \delta W_w 0.94 \times 10^{-9} \dots (36) \end{aligned}$$

where δW_w is the fractional portion of the wide-band beam intercepted by the array and $(I_\nu)_w^0$ = the number of neutrinos per pulse in the wide-band beam around the beam center.

Then:

$$N_{\mu w} = 10^{10} \times 0.29 \times 10^{-4} \times 0.94 \times 10^{-9} = 0.00027 \mu / \text{pulse} \dots (37)$$

For a detector 6 X larger (180 m) the rate increases to $1.4 \times 10^{-3} \mu / \text{pulse}$.

Discussion of the case of a narrow-band beam:

$$N_{\mu n} = (I_\nu)_n^0 \frac{3 \times 10^3}{3.3 \times 10^{12}} \delta W_n = \frac{(10^8) \times (0.94 \times 10^{-9}) \times (0.60 \times 10^{-2})}{10^0}$$

$$= 0.56 \times 10^{-3} \mu / \text{pulse}$$

These estimates are consistent with scaling the event rate from the Bubble Chamber site to the Lake Issyk-Kul target (6 Megaton). This gives $\approx 1.7 \times 10^{-3} \mu$'s per pulse (consisting of 10^{13} protons).

Daily Rates:

If the beam pulses are delivered every 15 seconds, and taking into consideration that in 1982 and 1983 the energy of the proton will increase about two and half times and since the cross section of the neutrino interaction is proportional to the energy, the rate will increase by at least two and a half times. This is because the multiplicity of charged particles giving rise to neutrinos slowly increases with energy (as $\log E$). Then the number of events to be detected will be increased at least linearly with the energy. We estimate that

$$N_{\mu n} = (2.5) \times .56 \times 10^{-3} \times 5.76 \times 10^3 \text{ pulses/day} \approx 8.1 \mu \text{ 's/day} \dots (38)$$

will be generated in the 1 megaton array. In the $(180)^3 \text{ m}^3$ full scale "calorimetric" array the rate is increased to $48 \mu \text{ 's/day}$.

Additional muons will be generated in the portion of the earth immediately below the lake bottom. Scaling the $(3 \rightarrow 10)$ u's per m^2 -pulse of 10^{13} 400Gev protons on the NØ target emerging from the berm at a point 1.4 km from the NØ target, will yield $1.1 \rightarrow 3.3 \times 10^{-8}$ u's per m^2 -pulse at Issyk-Kul 9,370 km from the NØ target. Hence over a detector area $(180 \text{ m})^2 \approx (19-62)$ u's per day should be observed emerging from the lake bottom for accelerator cycle times of 10 seconds and beam intensities of 1×10^{13} u's per pulse. A decay tunnel and a beam intensity 2.5x higher would tend to increase the rate to $120 \rightarrow 390$ u's per day.

The ratio f_μ of muons emerging from the lake bottom to the to the number of muons generated in the neutrino water target can be estimated by noting that the average energy of the interacting neutrinos is about 80 Gev (Figure 7-2) and about half the energy goes to the muon in the charged-current interaction. Hence, the effective lake bottom neutrino target thickness is the range of a 40 Gev muon in earth.

Thus the ratio f_μ is given by:

$$f_\mu = \rho_e R_\mu / \rho_w h \dots\dots\dots (38)$$

where: h is the height of the detector in meters.

ρ_e is the density of the lake bottom earth.

R_μ is the range of the 40 Gev muon in the lake bottom.

ρ_w is the density of water.

Taking the ionization loss of the muon as 2.2 Mev /gm/cm² in the lake bottom, $\rho_e = 3.0 \text{ gm/cm}^3$ as the density of the lake bottom earth and $h = 180 \text{ m}$ (the calorimetric version of BATISS) then:

$$f_\mu = 1.2 \dots\dots\dots (38)a$$

For thinner versions of the BATISS neutrino detector, the ratio increases as the inverse power of h. A thin array would be more efficient for detecting the charged-current component of the beam interactions but would not be able to observe the momentum dependence of neutrino oscillations.

In all of the versions of the neutrino detector the number of muons emerging from the bottom is greater than the array event:
 9.3) The Number of Interactions in the Detector from Solar Neutrinos.

By using a method analogous to that used to obtain equations (31) and (32) we can find the number of muons generated during

the period of a flare and detected by the underwater array. Instead of a beam of protons with a constant energy as is the case in an accelerator, the differential spectrum of protons in solar flares giving rise to muon neutrinos is a power law spectrum $dN = KN_p^0 E^{-\gamma} dE$. These protons produce neutrinos in the solar atmosphere in nuclear interactions.

The number of muons, N_μ , generated by the high energy solar neutrinos and detected in the water target is [1]:

$$d(dN_\mu(E_\mu)) = \frac{dN_\nu(E)}{dE} \frac{N_\mu(E_\mu)}{N_\nu(E_\nu)} \frac{S_{\text{det}}}{4\pi R_{\text{solar}}^2} (\ell + h_{\text{det}}) \sigma_\nu N_A dE_\nu$$

where

$$E_\mu = \frac{1}{2} E_\nu; \text{ and } N_\mu \approx 10^{-32} N_p^0 \text{ when the spectral index,}$$

$$\gamma = 3 \text{ and } N_\mu \approx 10^{-34} N_p^0 \text{ when } \gamma = 5. \dots \dots \dots (39)$$

where ℓ = path of muons in the ground target, h is the height of the detector and $N_A = 6 \times 10^{29}$ is the total number of nucleons/m³ in the water target detector.

For flares in which the number of high energy protons generated is $N_p \approx 10^{33} \rightarrow 10^{34}$, between one to one hundred neutrino events will be detected respectively.

It has been estimated that the frequency of such solar flares is about one per year [1].

10.) Background.

10.1) Muon Cosmic-Ray Background.

The dependence of the muon beam intensity on the thickness of earth traversed has been studied by several groups [19]. At a depth of 500 meters of water the intensity of cosmic-muons is

$$dN_{\mu}(5 \times 10^4 \text{ gr/cm}^2) = 7 \times 10^{-6} (\text{cm}^2\text{-sec-str})^{-1}$$

In a detector of area $S = 10^8 \text{ cm}^2$, the rate is:

$$N_{\mu} = 7 \times 10^2 \mu\text{'s}/(\text{sec-str.})$$

for an area, $S = 3.4 \times 10^8 \text{ cm}^2$:

$$N_{\mu} = 2.4 \times 10^3 \mu\text{'s}/(\text{sec-str.}).$$

Taking into account the fact that fluxes of muons of cosmic-ray origin, including those generated by cosmic-ray neutrinos, will be distributed uniformly in time whereas the neutrino beam from the accelerator is time modulated such that its charged-current muons can be gate-selected allows almost complete elimination of the cosmic-ray background.

10.2) Neutrino Background.

The limits of the cosmic-ray neutrino background for ν_{μ} are shown in Table 10.1 [19].

Table 10.1 Flux of Neutrinos from Cosmic-Rays

$E_{\nu_{\mu}}$ (MeV)	Flux $(\text{cm}^2/\text{sec})^{-1}$
≥ 100	$\leq 7 \times 10^{-4}$
$\geq 1,000$	$\leq 5 \times 10^{-6}$
$\geq 10,000$	$\leq 5 \times 10^{-9}$

The flux of cosmic-ray neutrinos is about the same as the flux of cosmic-ray muons. The flux of antineutrinos would usually be less than that of neutrinos and in any case would not exceed the bounds in the table. The flux from

the beam over a 20 μ s (single turn fast spill at FNAL) time gate will be many orders of magnitude larger. This can be seen from a comparison of the spectrum of accelerator neutrinos, Fig. 7-3, with the spectrum of cosmic-ray neutrinos given by 40.a,b,c,d below.

The standard spectrum of cosmic-ray neutrinos is approximated by the following analytical forms [19]:

$$I_{\pi_\nu}(E_\nu) = \begin{cases} 1.85 \times 10^{-2} (0.08 + E_\nu)^{-2.8} & (1 \rightarrow 10\text{GeV}) \dots (40.a) \\ 6.65 \times 10^{-2} (1.1 + E_\nu)^{-3.2} & (10 \rightarrow 100\text{GeV}) \dots (40.b) \end{cases}$$

$$I_{\mu_\nu}(E_\nu) = \begin{cases} 7.65 \times 10^{-2} (0.37 + E_\nu)^{-3.75} & (1 \rightarrow 10\text{GeV}) \dots (40.c) \\ 1.48 \times 10^{-2} (3.5 + E_\nu)^{-4.5} & (10 \rightarrow 100\text{GeV}) \dots (40.d) \end{cases}$$

where $I_{\pi_\nu}(E_\nu)$ and $I_{\mu_\nu}(E_\nu)$ are the differential spectra (in units of the number of neutrinos/($\text{cm}^2\text{sec-str-GeV}$) which rise from π and μ decay respectively.

10.3) Natural Radioactivity Background

This background is generated by the Cherenkov light produced by decay products of trace radioactive elements dissolved in the lake water. It is produced either directly by electrons from Beta decay or by Compton scattered electrons. The radioactive background can be greatly reduced by requiring two or three-fold coincidences among adjacent modules. The probability of chance coincidence is small because the natural radioactivity of the lake is not great. Further discussion of the natural radioactive background due to specific isotopes is given in reference [27].

11.) Synchronization of Detector and Neutrino Source Clocks

During the winter and spring of 1981 the BRISK-BATISS Neutrino Telescope at Western Washington University was operating with a source-detector event clock synchronization of ± 18 ms. An inexpensive technique was developed to transport time using the telephone. This level of accuracy is theoretically useful in reducing background in the telescope due to chance coincidence by single cosmic-rays to about 1 event per year for four-fold coincidence events. Rates (≈ 50 /day) of four-fold coincidence events were observed, most of these are due to air showers. Large variations have been observed depending on whether the FNAL or the BNL accelerators were operational. These results of the feasibility study are discussed in the attached paper "Search for Neutrino-Like Events 2,750 km from the Source" (their exact nature is, however, unknown) which reports an excess of about a few neutrino-like events per day when the FNAL is operating.

11.1) Synchronization Constraints for the Experiment.

Since most of the electronic modules chosen for this experiment have about one nanosecond rise time ability, a system of recording clocks, drifting by no more than one nanosecond in-between times of checking of readings of source and detector clocks, are needed to optimize the physics. If the checks are made once daily then clocks with a stability $\delta t/t = 1.2 \times 10^{-14}$ must be used. If the stability is better than 10^{-14} longer intervals between checks are possible--a highly desirable situation.

The initial feasibility studies were carried out with the assistance of Carroll O. Alley and his Quantum Electronics Group of the University of Maryland. We feel confident that, properly funded, the necessary levels of stability can be achieved by their group in this experiment.

11.2) Mass of Heavy Neutrinos from Delays in Transit Time.

Let t_γ be the transit time for a particle traveling at the speed of light. Assume that a neutrino, under study, has rest mass E_0 and therefore will travel with a velocity v which is slower than the speed of light in a vacuum. As usual let $\beta = v/c$. Let L be the distance between the neutrino detector and the neutrino source.

Then the relation between the transit time t_γ of a heavy and t_γ of a massless neutrino between the same two points is:

$$t_{\nu} = \frac{t_Y}{\beta} \dots \dots \dots (41)$$

Then the difference in the transit time Δt between the heavy neutrino and the massless neutrino is:

$$\Delta t = t_{\nu} - t_Y = \left(\frac{1}{\beta} - 1\right)t_Y \dots \dots \dots (42)$$

In this experiment we propose to measure Δt and derive or place an upper limit on the mass of a heavy neutrino. Once Δt is measured β can be found from (42) above. However β is related to the rest mass of the neutrino and its total energy by the relationship:

$$\beta = \sqrt{1 - (E_0/E_{\nu})^2} \dots \dots \dots (43)$$

where E_{ν} is the energy of the neutrino which can be determined from the measurement of the hadronic shower and the energy of the muon (from the range and from secondary electromagnetic interactions) and can be as low as the minimal detectable energy of the neutrino. Let E_0/c^2 be the rest mass of the heavy neutrino.

In the case where $E_{\nu} \gg E_0$ we obtain by a Taylor series expansion of (43) and use of (42):

$$\Delta t \approx \frac{t_Y}{2} \left(\frac{E_0}{E_{\nu}}\right)^2 = \frac{L}{2c} \left(\frac{E_0}{E_{\nu}}\right)^2 \dots \dots \dots (44)$$

For a chordline distance of 9,370 kilometers, a tau neutrino with energy $E_{\nu} = 2$ GeV, and a rest mass $E_0 = 10$ MeV we have a very long delay, viz.:

$$\Delta t(\text{ns}) = 390\text{ns} \dots \dots \dots (44a)$$

A 500 KeV rest mass neutrino with 2 GeV total energy will lag 1 ns behind a bucket at the location of Issyk-Kul.

In general, solving (44) for E_0 we have

$$E_0 = E_\nu \sqrt{\frac{2c\Delta t}{L}} \quad (45)$$

Insofar as the uncertainties in the measurement of E_0 , E_ν , Δt and L are small compared to the quantities themselves then the fractional error in E_0 is given by the relation

$$\frac{\delta E_0}{E_0} = \frac{\delta E_\nu}{E_\nu} + \frac{1}{2} \frac{\delta \Delta t}{\Delta t} - \frac{1}{2} \frac{\delta L}{L} \quad (45a)$$

Here, the error $\frac{\delta E_0}{E_0}$ depends on the errors on the right and the latter are dependent on the muon and hadron shower energy determinations, time measurements, beam conditions and geodetic measurements.

In general we will measure $t_{0\ell}$ the time difference of the event from the nearest bucket. However, the true transit time difference will be:

$$\Delta t_\ell = t_{0\ell} + \ell T_{RF} \quad (45b)$$

where ℓ is an integer to be determined and $T_{RF} = 18.3$ ns the Radio Frequency period--the time between buckets. The Δt of a second interaction, which falls out of the bucket time window, will be given by:

$$\Delta t_n = t_{0n} + n T_{RF} \quad (45c)$$

If the beam consists of only one heavy neutrino, both events must give the same E_0 in equation (45). Equating the two solutions to (45) we can find the integers n and ℓ by solving the following equation:

$$n = a + b\ell \quad (45d)$$

where a and b are determined from the experiment and are given by:

$$a = (E_{\nu l}/E_{\nu n})^2 (t_{ol}/T_{RF}) - (t_{on}/T_{RF})$$

$$b = (E_{\nu l}/E_{\nu n})^2$$

The smallest pair of integers l and n satisfying (45d) is taken as the solution to (45d) which in turn gives the transit time delay from equations (45b) and (45c). The transit time delays thus determined give the mass of the heavy neutrino from equation (45).

12.) Cherenkov Light Detection.

12.1) Transparency of Lake Issyk-Kul.

The water of Lake Issyk-Kul is famous for its "saturated" blue color. This implies, first of all, that the lake does not contain yellow matter, and secondly, that there is not a great quantity of suspended particles. It is known that both the yellow matter and other suspended matter provide strong absorption in the blue parts of the spectra [16]. Consequently, absorption of Cherenkov light in Issyk-Kul's water is not great. It is possible to consider the "optical transparency" of the water to be about that of distilled water, that is, the coefficient of absorption is about $C = 0.02 \text{ m}^{-1}$ for $\lambda = 476$ nanometers (the average wavelength for Cherenkov radiation).

Information about transparency is obtained with the help of the Secchi disk. Measurements show that the coefficient of attenuation of light in water, through scattering and absorption, is not great. In reference [17], the relationship between the absorption of light, in units of "e", and the depth Z of

disappearance of the disc is written as:

$$Z = \frac{0.15}{\lambda \nu} \dots \dots \dots (46)$$

By the scale of V. V. Shulekina for Issyk-Kul $\nu \approx 3$. Then the coefficient is calculated by Equation (46) and found to be 1.1, and for Issyk-Kul will give the exponential coefficient of absorption of light as:

$$K_n = \frac{1.1}{Z} = \frac{0.04}{\text{meter}} = 0.04\text{m}^{-1} \dots \dots \dots (47)$$

In reference [18] it is shown that the Secchi disc disappears behind upward scattered light. Therefore, equation (47) gives the coefficient " K_n ", which determines the absorption coefficient of light from dispersion, and the exponential attenuation coefficient " K ". The attenuation coefficient becomes $K = 0.06\text{m}^{-1}$ and the corresponding attenuation length is:

$$\frac{1}{K} = \frac{1}{0.06} \approx 17 \text{ meters} \dots \dots \dots (48)$$

Results of an expedition to Lake Issyk-Kul in 1980 to determine the absorption of light in its water showed that the beam attenuation length was 15 meters to 21 meters, at depths from 10 meters to 650 meters.

The absorption of light is weakly dependent on depth. For depths of 150 meters to 600 meters the coefficient of absorption practically remains constant. The source of light was a light emitting diode. The radiated light had a wavelength the same as the average wavelength of Cherenkov light.

A photomultiplier, model FEY 49, was used to detect the photons. A schematic of the instrument which was used to measure

the transparency of the water is shown in Figure 12.1. "a" = the schematic of the module, "b" = the block diagram of the electronic and electrical parts, "c" = a longitudinal cut of the cable.

12.2) Photomultiplier Sensitivity to Cherenkov Light.

Cherenkov radiation may be measured by photomultipliers distributed in the lake water. In the large, recent models, the minimum detectable flux of Cherenkov light approaches $(n_\gamma)_{\min} = 0.08 \text{ photons (cm}^{-2}\text{)}$ to $0.03 \text{ (cm}^{-2}\text{)}$. For example, the type FEY 495 photomultiplier made in the USSR, is sensitive to a flux as low as $0.08 \text{ photons/cm}^2$. The more recent RCA 4522, made in the USA, is sensitive to $0.03 \text{ photons/cm}^2$.

We now estimate the flux of Cherenkov light generated by the muon and the hadronic shower components of the neutrino interaction. Let E_h be the energy in GeV of the hadronic shower and let E_μ be the energy in GeV of the muon. Referring to figure 12.1-2 estimates of the flux of photons from the muon N_{γ_μ} (photons/cm²) and the flux of photons from the hadronic shower N_{γ_h} (photons/cm²), are given by Equations (49) and (50).

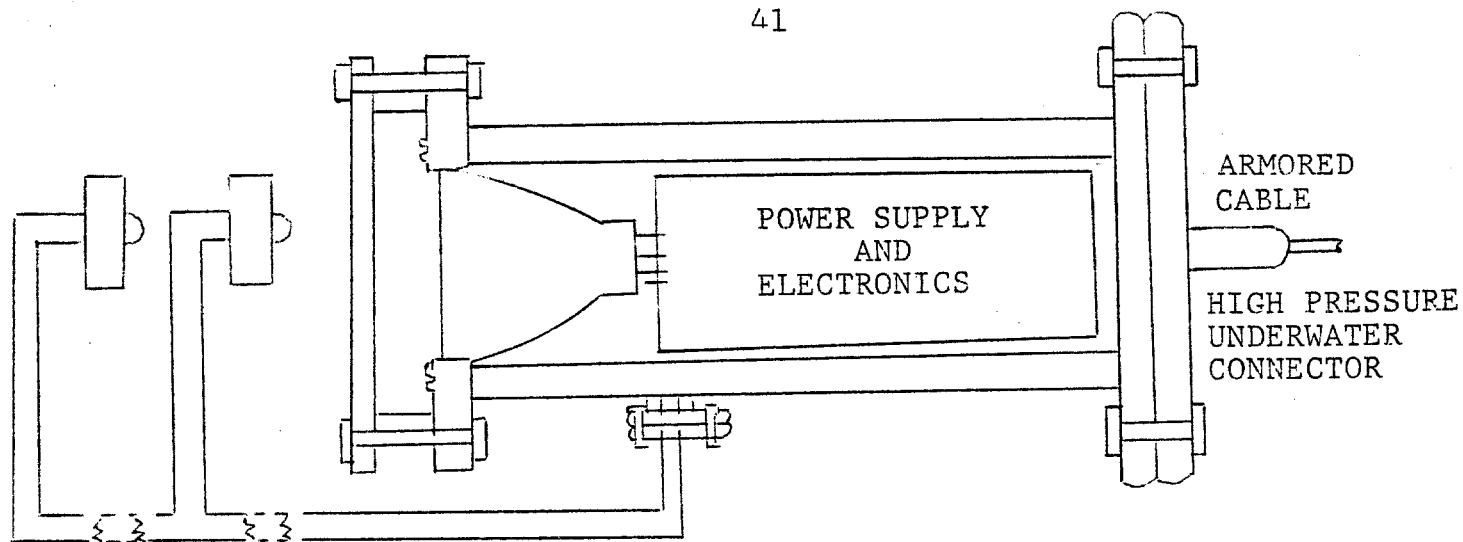
$$N_{\gamma_\mu} = L / (2 \pi \tan^2 \theta_c D_\mu) \quad \dots \dots \dots (49)$$

where L is the number of Cherenkov light photons emitted per unit path length of the muon,

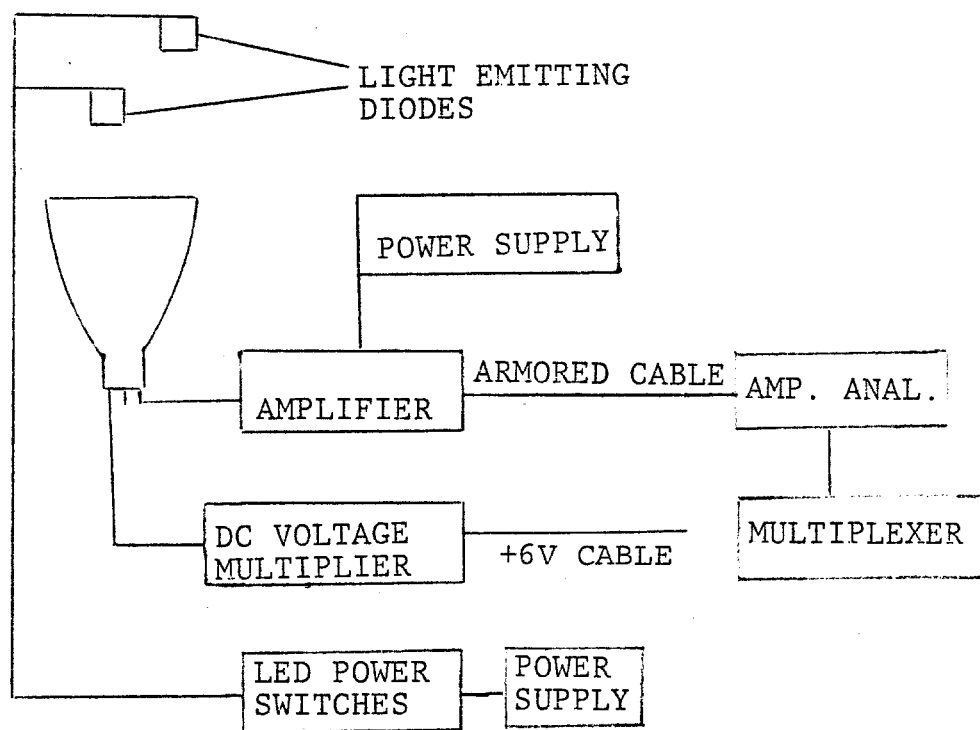
θ_c the angle between the muon trajectory and the direction of the photon,

D_μ is the impact parameter of the muon.

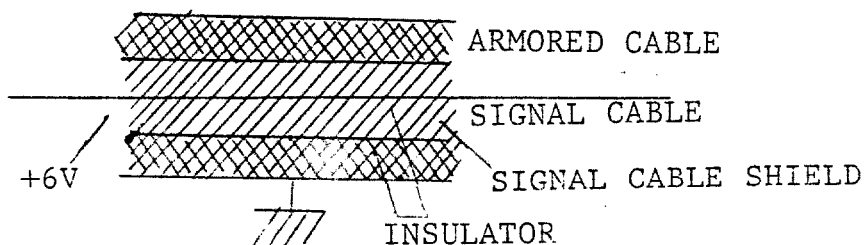
$$N_{\gamma_h} = LE_h(\text{GeV}) \sin^2 \theta_c / (pE_1(\text{GeV}) 2\pi D_h^2 \Delta\theta) \quad \dots \dots \dots (50)$$



"a"



"b"



"c"

Figure 12.1
SCHEMATIC OF WATER TRANSPARENCY MEASUREMENT EXPERIMENT

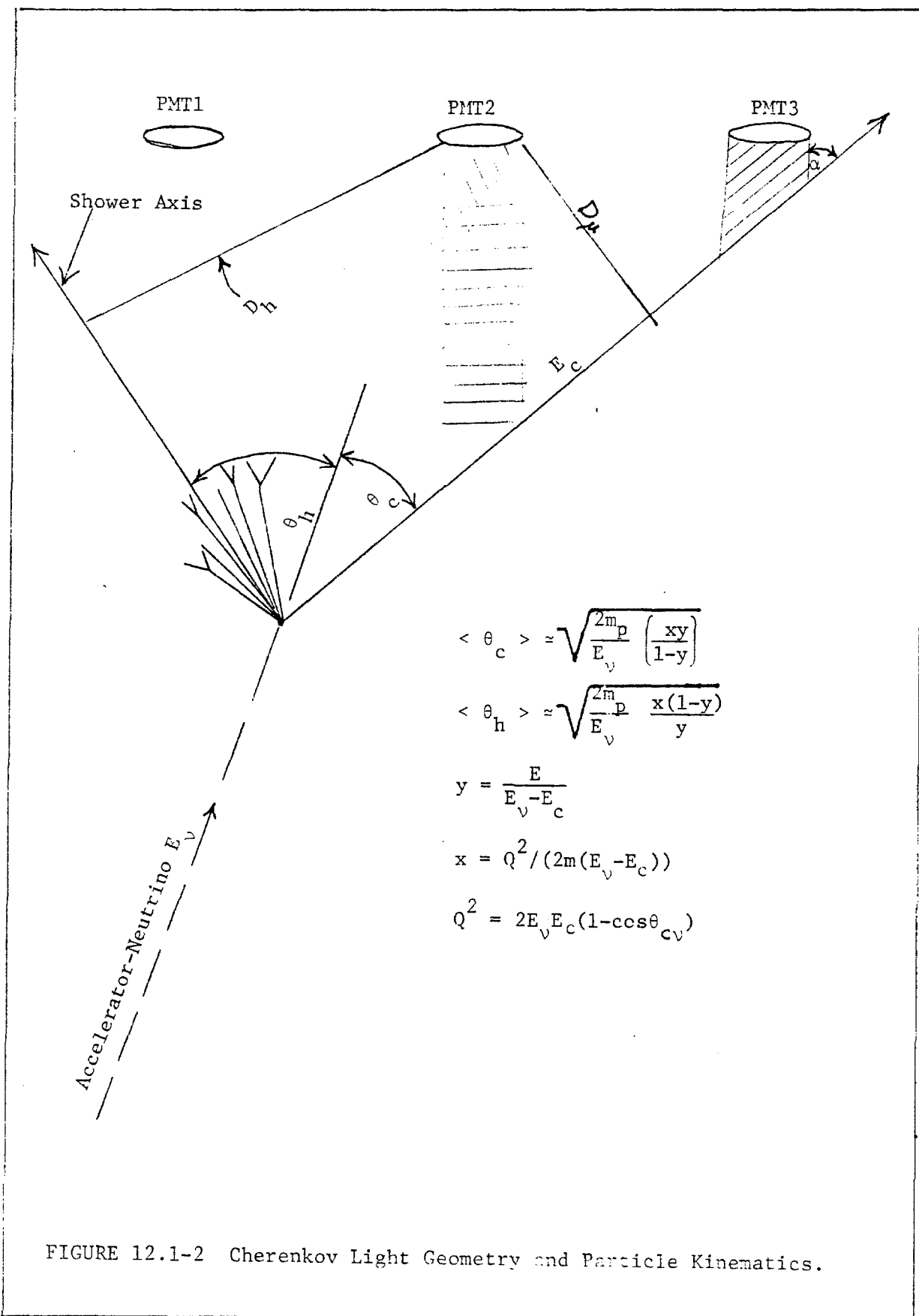


FIGURE 12.1-2 Cherenkov Light Geometry and Particle Kinematics.

where E_i is the ionization loss for relativistic particles in water:

p is the density of water,

$\Delta\theta$ is the angular spread in the Cherenkov light generated by the hadronic shower in water.

D_h is the impact parameter for the shower.

Assuming $L = 200$ photons/cm:

$$p = 1 \text{ gram/cm}^3$$

$$E_i = 2 \times 10^{-3} \text{ GeV/(g/cm}^2\text{)}$$

$$\Delta\theta = 0.2 \text{ radians}$$

we have:

$$N_{\gamma\mu} = (35/D_\mu) \text{ photons/cm}^2 \dots\dots\dots(51a)$$

$$N_{\gamma h} = (53 \times 10^3 E_h/D_h^2) \text{ photons/cm}^2 \dots\dots\dots(51b)$$

Equations (51.a) and (51.b) are good approximations to the flux of photons up to the attenuation length of Cherenkov light in Issyk-Kul water.

Equation (51.a) is valid for low energy muons from accelerator neutrino interactions. For the cosmic-ray muons with $E_\mu \geq 1,000$ GeV, generation of Cherenkov light from electrons and electron positron pairs from bremsstrahlung and direct pair production processes must be taken into account.

Coincidence techniques can be used to separate Cherenkov light from the random signals from the background of residual sunlight at depths around 500 meters in Lake Issyk-Kul. Further, the lake has no known bioluminescent organisms to produce additional background which is important in underseas detectors.

13.) The Detector.

13.1) The Location of the Detector.

Batavia is located about 30 miles west of Chicago and has the following geographic coordinates:

$$\lambda = 41^{\circ} 50' \text{ N, and } \phi = 88^{\circ} 15' \text{ W.}$$

Lake Issyk-Kul is located in the Tien-Shan mountains and is about 70 kilometers from Alma-Ata. The surface of the lake is at an elevation of 1609 m. above sea level. The staging area has the following geographic coordinates:

$$\lambda \approx 42^{\circ} \text{ N, and } \phi \approx 78^{\circ} \text{ E.}$$

The through-the-earth cord line distance between Batavia and Issyk-Kul is 9,370 kilometers. The trajectory goes through intermediate layers of the earth but does not, unfortunately, touch the core. The distance of closest approach to the center is $4.8 \times 10^3 \text{ km}$ [3]. The average density of earth along this path equals about 4 grams/cm^3 (in the core the density is $8 \rightarrow 11 \text{ grams/cm}^3$), and the average thickness of the matter traversed is about $3.7 \times 10^9 \text{ grams/cm}^2$. A calculation utilizing the charged-current interaction cross-section of neutrinos with nucleons shows that 0.1% of the neutrinos are absorbed. About 0.03% are scattered out by the neutral-current interactions. The time of flight of the neutrino is 0.0312 seconds.

The maximum depth of Issyk-Kul is a little greater than 700 meters; the water contains a small quantity of suspended matter; the lake does not freeze. More than 1/3 of the surface area of the lake covers water depths greater than 500 meters. At the southern shores near the local ports of Akterek, Koltsovka and

almost to Tamgi, deep water fields are located only 4 - 8 kilometers from the bank.

The railway runs up to the Lake Port Ribachi (about 30 km from Tamgi, the planned staging area for BATISS). There are also motor roads and air transport to Port Ribachi. From Port Ribachi to any place on the lake there is complete water access by large ships and also paved roads.

13.2) Module for the Detection of Muons at Large Depths Under water.

13.2.1) Soviet Version.

In reference [3] the results are shown from a Soviet module which was used to measure the transparency of water and intensity of background radiation of Lake Issyk-Kul. Figure 12-1 is a diagram of the Cherenkov Light Detector module used to carry out these measurements. The figure shows the following elements:

- 1) photoelectron multiplier.
- 2) electronic diagram of amplification and pulse former.
- 3) high voltage multipliers.
- 4) electrical power supply.
- 5) amplitude analyzer.
- 6) timing organization.
- 7) information storage.
- 8) remote programming and control.
- 9) the module and additional equipment for the measurement of the transparency of water using light emitting diodes.

13.2.2) The American Versions.

a) The first version is a sphere made of borosilicate glass. The module can be dismantled into hemispheres and is shown in Figure 13.2-1.

b) The second version is a metal-glass module in a cylindrical form. The cylindrical module contains three photomultipliers, and information from each photomultiplier is collected upon a pre-selected coincidence among the photomultiplier tubes in the casing.

Figure 13.2-2 shows the layout of the cylindrical module. From an examination of the various designs of neutrino detector modules we find that the module with the largest optical area is spherical or cylindrical with hemispherical caps. In this form a cylindrical design with an opaque partition between the two clusters of three photomultipliers (looking in opposite directions) is used. Such a module is depicted in Figure 13.2-3. The advantage of a cylindrical module is the simultaneous and independent detection of the neutrino particle by the lower hemisphere and the cosmic-rays by the upper hemisphere.

Using a three-fold coincidence among the lower or the upper photomultipliers as a trigger will nearly eliminate events due to the dark current electronic noise of the photomultiplier. Furthermore, the three photomultipliers increase the reliability of the module and allow an accurate calculation of the detection efficiency of each photomultiplier tube [20].

A working trigger signal from a module will consist of a two-fold majority coincidence between any two photomultipliers in the

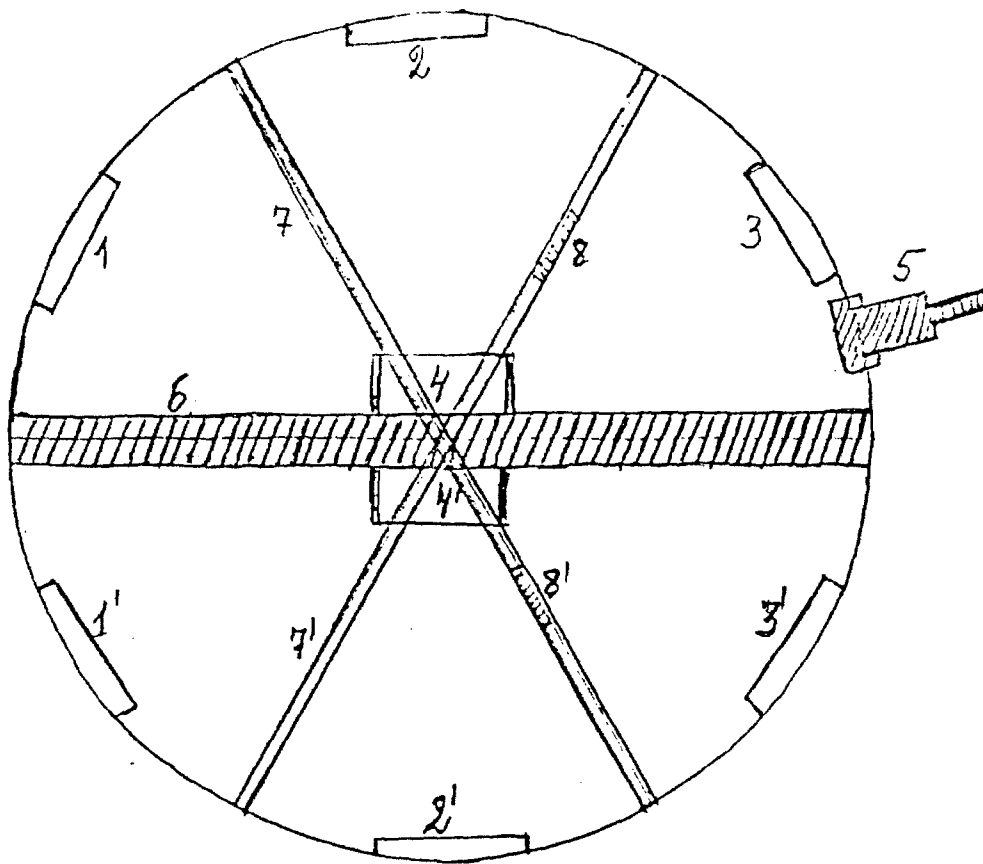


Figure 13.2-1 Schematic of a Spherical Module

- 1', 2', 3', 1, 2, 3 - Photomultipliers
- 4', 4 - Electronic Circuits
- 5 - Electrical Penetrators
- 6 - Water Gaskets
- 7, 7' - Holding Bands
- 8, 8' - Turn Buckles

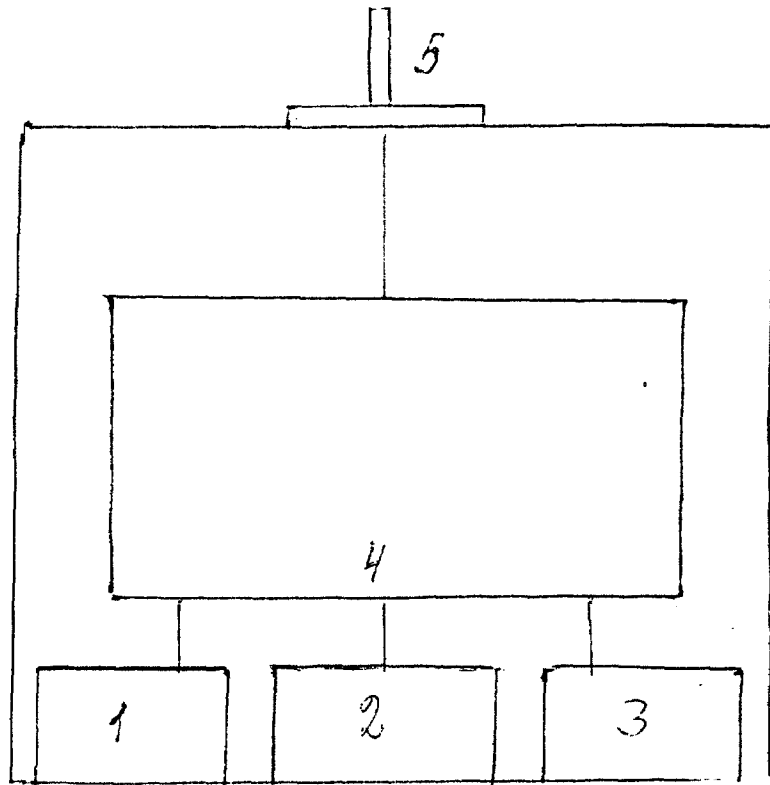


Figure 13.2-2 Schematic of a Cylindrical Module

- | | | |
|---------|---|------------------------------|
| 1, 2, 3 | - | Photomultipliers |
| 4 | - | Module Electronics |
| 5 | - | Signal and Power Penetrators |

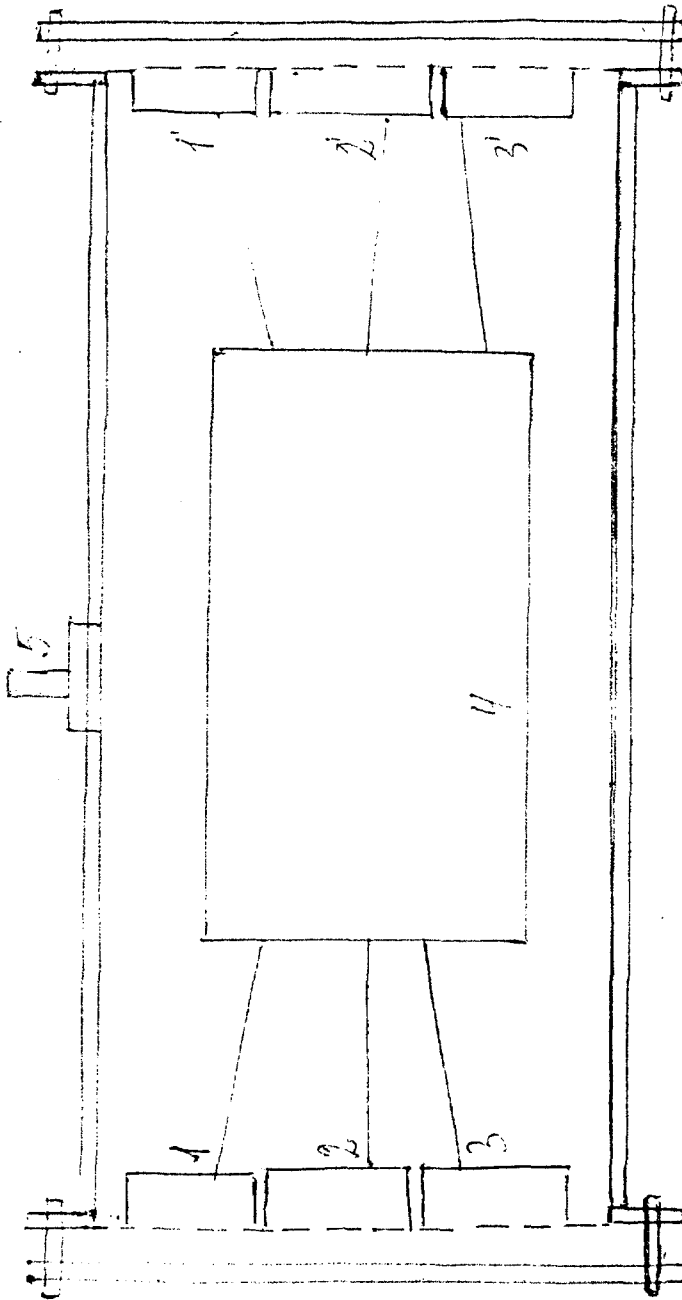


Figure 13.2-3 Schematic of a Two Way Module

- | | | |
|------------|---|--|
| 1, 2, 3 | - | Upward Looking Photomultipliers |
| 1', 2', 3' | - | Downward Looking Photomultipliers |
| 4 | - | Electronics |
| 5 | - | High Pressure Power and Signal Cable Penetrators |

module which point in the same direction. The probability of a noise signal from two-fold coincidence (within a 3 ns time interval) among any of the three photomultipliers in one module is relatively small: the order of 0.3 per second if the tube rates are running at 10^4 Hz. In addition, the requirement of a coincidence between adjacent modules reduces the noise events to about one per year. The cosmic-ray muons are expected to trigger the module at a rate of 15 Hz.

(13.3) The Number of Modules in the Neutrino Detector.

The maximum spacing between the modules may be established from the minimum detectable fluxes of the photomultipliers to be used in the array. The detectable fluxes of the Cherenkov light depend on the impact parameter, the azimuthal and polar angle of the particle and the attenuation length of the various components of the Cherenkov light in Issyk Kul water. For conditions when $D < \beta$ (the attenuation length of light) and the particles are parallel to the normal of the face of the photomultiplier tubes, we estimate D , the spacing of the module in the array.

For photomultiplier tubes with a threshold:

$(N_\gamma)_{\min} = .03$ photon/cm² and hadronic showers of energy

$E_h = 40\text{GeV}$ we have:

$$(D_\mu)_{\max} = (35/.03)\text{cm} = 12 \text{ meters} \dots \dots \dots (52)$$

$$(D_h)_{\max} = (53 \times 10^3 E_h /.03)^{1/2} \text{cm} = 84 \text{ meters} \dots \dots \dots (53)$$

For photomultiplier tubes with a threshold $(N_\gamma)_{\min} = .08$ photons/cm² and hadronic showers of energy $E_h = 40\text{GeV}$ we have:

$$(D_{\mu})_{\max} = (35/.08)\text{cm} = 4.4 \text{ meters} \quad (52a)$$

$$(D_h)_{\max} = (53 \times 10^3 E_h /.08)^{1/2} \text{cm} = 52 \text{ meters} (53a)$$

Since three photomultipliers are to be located in each module in the detector the maximum detectable distance for muons is increased by a factor of three in equations (52) and (52a). If the spacing of the modules is set by requiring "certain" detection of the muon then the shower component will be easily detected. We note, however, that Equations (53) and (53a) overestimate the maximum detectable impact parameter since the parameters are much greater than the attenuation length. Future calculations will take into account the effects of attenuation lengths and their dependence on the wavelength, and specific photomultiplier design. This information will be useful in reconstructing the shower axis and shower brightness in order to estimate E_h and θ_{ν_h} (the angle between the incident neutrino and hadronic shower axis).

13.4) Geometry of the BATISS Detector.

The geometrical layout of the detector must be such so as to be easily assembled and disassembled. A lightweight hexagonal structure with modules located at each of the vertices and one in the center are planned as the basic structural elements of the detector. The hexagonal section is constructed of three triangular frames fastened between themselves with intersection

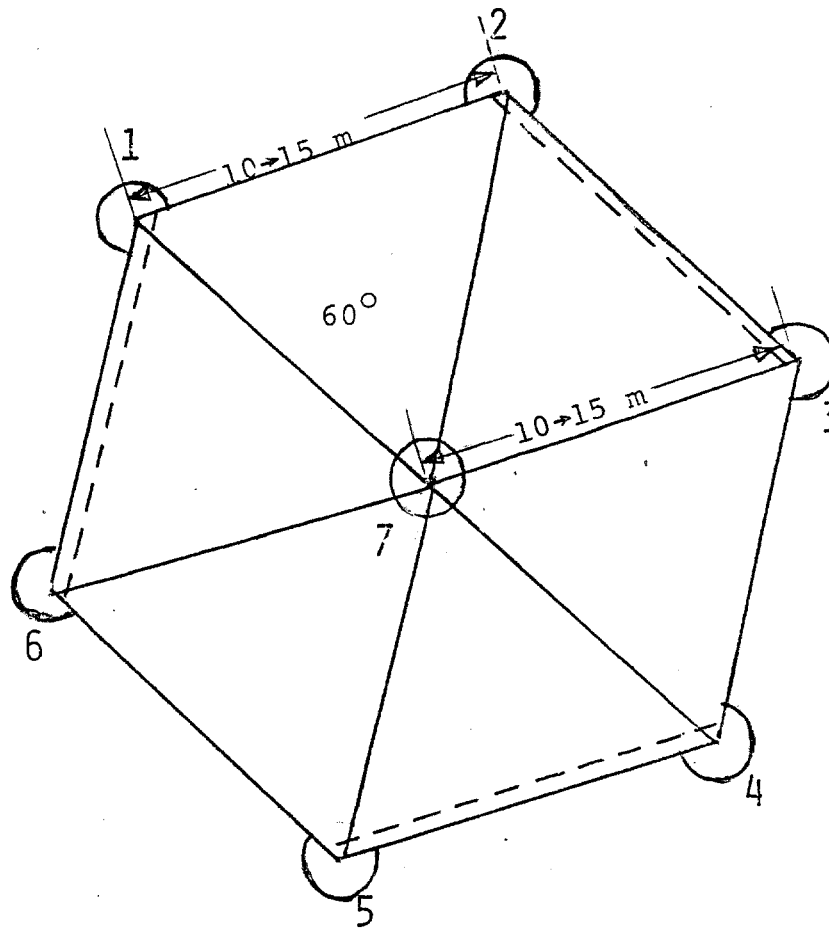


Figure 13.4

Schematic of a Section (Within a Ganglion).
A Section is Composed of 7 Modules.

1, 2, 3, 4, 5, 6, 7 - Modules

1-3-4; 1-5-6; 1-2-7 - Triangular Construction Elements

2-3; 4-5; 6-7 - Ribs Joining the Triangular Elements

Total Rib Length = $12 l_o = 180 \text{ m}$

Number of Interfaces = 7

For $l_o = 15 \text{ m}$

Geometrical Area $A_g = 585 \text{ m}^2$

One Neutron Sensitive Area $A_s =$

$$3 \times \pi \times (15 + 12)^2 = 6,621 \text{ m}^2$$

Geometric Volume:

$$V_g = 2 \pi \times 2/3 A_g = 165,180 \text{ m}^3$$

fasteners as is shown in Figure 13-1. Each arm, a hollow tube which may be used for carrying the signal and power cables, is equal to the length of a "rib" of the hexagon.

The entire array consists of 108 hexagonal sections. Each section will have a maximum sensitive area for detection of muons in the amount of $6,362 \text{ m}^2$ (a circle of radius 45 m). The geometrical area of the section is 675 m^2 . They can be assembled into an array in several ways.

The length of the hexagon's ribs is determined by the weakest signal sought in the detection of muons of low energy, such as those generated by the interaction of solar muon neutrinos with water.

The clarity of the water coupled with the design of the module suggests a spacing (rib length) of 10 to 15 meters.

The following four variants of the groupings of the sections are considered:

- 1) 18 Gangleons each with 6 layers of hexagonal sections.
- 2) 27 Gangleons each with 4 layers of hexagonal sections.
- 3) 12 Gangleons each with 9 layers of hexagonal sections.
- 4) 9 Gangleons each with 12 layers of hexagonal sections.

So it will be necessary in any case to manufacture 108 hexagonal sections. Since there are seven modules in every section, the array will consist of a total of 756 modules. Hence, the array will consist of 2,268 upward looking photomultipliers, and a like number looking downward.

13.5) Calibration of Location of Modules.

To utilize the 18 ns rf structure of the beam in a search

for heavy neutrinos and to study geophysical phenomena it is necessary to know the absolute location of the modules. While the supporting structure is "rigid" it is expected to settle with time and therefore it is necessary to monitor the positions of all of the modules. The absolute location of the modules will be accomplished by three separate calibration procedures which are to be followed in the experiment. They are described in the following sections.

13.5.1) Geometrical Location of the Modules.

At the time of the detection of a neutrino interaction it is necessary to know the positions of all of the modules to an accuracy of less than two centimeters relative to a set of fixed bench marks driven into the bed rock beneath the detector. Since the array is "rigid," position transducers need be placed on only a small number of widely distributed modules. Either sharp light or acoustical pulses will be transmitted then received from benchmarks. The transit time of the pulses to the respective modules can be used to determine the coordinates of the module.

13.5.2) Electronic Transit Time.

The voltage between the face of the tube and the first dynode must be held to a high level and isolated from variations imposed on the remaining dynodes, in order to hold the pmt signal transit time constant while being able to independently adjust the overall gain of the photomultiplier. A set of strategically placed "bluish green" light emitting diodes are to be used to help check

on the electronic transit time of photomultiplier signals in each of the modules.

13.5.3) Consistency Checks.

Cosmic-ray muons passing through the array can be used to monitor the relative geometrical and electronic position of the modules. On the average the muons will define straight line trajectories and the times of arrival of the Cherenkov light pulses can be used to calculate the pmt "electronic" signal delay and the relative geometrical locations which are required to yield straight line fits to the muon trajectory.

13.6 Detector Components.

13.6.1) Programmable High Voltage Sources.

The high voltage for the photomultipliers is obtained from a low voltage electrical feed to the photomultipliers, which is then converted by means of a transformer to the high voltages required to operate the pmt. One low voltage power cable supplies the six photomultipliers in every module. Photomultipliers of the type FEY-49 or of the type RCA-4522 are used in the current prototype modules. For both of these types of photomultipliers high voltage from 1,700 to 2,500 volts are necessary. Both modules have been tested and operated to 2,000 foot depths of water. One was successfully tested in the Fermilab NØ beam line.

The necessary current required to supply the photomultipliers is dependent on the voltage thresholds required to operate the discriminators and coincidence circuits. About 0.1 ma to 0.3 ma per pmt is required for the contemplated electronics. In such a

manner six photomultipliers will draw .6 to 1.8 ma of DC current. On the average the high voltage on the photomultiplier is about 2,000 volts. From this it follows that using one high voltage transformer per module, it must operate at a power level from 1.2 to 3.6 watts, or on the average of 3.0 watts. (In the USA off-the-shelf high voltage DC transformers of the type VENUS satisfies these demands.)

13.6.2) Underwater Transmission Cables.

The current BATISS test telescope uses "hard wired" techniques to select particles from the FNAL. This requires a substantial amount of cable. While our designs can be directly expanded to the large underwater array, it may be more efficient (if practical) to consider alternate techniques. Some general requirements are developed for such a new system in the paragraphs below.

13.6.2-1) Interfaces.

The interfaces for the connections of module outputs to underwater transmission cables and the various other array components (such as the module's cables to the minicomputers) must meet the following criteria:

- 1) They must be capable of easy connection and disconnection in the field.
- 2) The interconnection must be capable of operating under pressures of no less than a 1,000 meters of a column of water.
- 3) The interface must be able to connect several photomultiplier cables in one operation.

13.6.2-2) Electrical Conductors.

The underwater cable must carry an electric current for supplying power to the photomultipliers and the data acquisition module, and it must also contain the signal transmission line for information from the module to the minicomputer. This would require a four conductor cable where every conductor is isolated and shielded.

The following information must be transmitted by the cables:

- 1) Signals transmitted from each photomultiplier to the computer. One is used to measure the amplitude of the Cherenkov light, a second the time of arrival. Using the time of recording of the light pulses, information from the other two photomultipliers, a coincidence requirement can be established so as to exclude background signals from the photomultipliers.

- 2) Signals from the coincidence unit in the module are fed to a minicomputer.

- 3) A signal must be transmitted conveying the address to the module.

- 4) The electrical power will be supplied by a separate and fourth conductor.

13.6.2-3) Optical Cables.

This version utilizes laser diodes which transmit light over an optical cable. Optical cables exist which can transmit the necessary information for 2 km; electrical shielding for these conductors is not necessary.

13.6.2-4) Information Transmission Cables.

The cable transmitting information from the minicomputer to the on-shore data analysis computer must have three lines: (1) to supply the electrical power; (2) to carry information, (3) to control the minicomputers, which in turn control the module status.

13.6.2-5) Interconnection Cables within a Section.

The cable from every section to the minicomputer must have a minimum of 28 leads unless multiplexing can be carried out at the central module of a section.

13.6.2-6) Total Cable Length for the Array.

The amount of cable required for the operation of the detector array depends on the specific system chosen for the transmission and multiplexing of the data. Several systems are under consideration. The minimal amount of signal transmission cable is given by the following.

1) The cable from the shore to the minicomputers is 20 km (array to shore) x 9 (gangleons) = 180 km.

2) The cable from each section to the computer is 1,500 meters for one gangleon. Therefore, 1.5 km x 9 (number of gangleons) = 140 km.

3) For each section it is necessary to have a minimum of 105 meters of cable. Altogether the BATISS neutrino detector is composed of 108 sections. For all the sections it is necessary to have 11.34 km of cable for the section plus interconnection between sections amounting to 233 km of cable.

4) In every module there are six photomultipliers. Altogether there are 4,536 photomultipliers. Each photomultiplier requires 3 meters of co-axial cable. Therefore, the total length of cable required for all modules is

$$L = 4,536 \text{ (photomultipliers)} \times 3 \text{ (co-axial cables)} \approx 14 \text{ km}$$
of cable. Thus about 440 km of signal quality cable are needed for the array.

5) In the neutrino telescope now operational at Western Washington University, selection of signals with a proper time sequence corresponding to through-the-earth events is not carried out by computer software as planned for BATISS, but by means of insertion of calibrated delay cables into the lines leading to the coincidence unit. These "trim" delay lines make the signals which are generated by a muon from the direction of the FNAL arrive simultaneously at the coincidence unit. The coincidence unit then provides the master trigger for the TDC and the ADC start gates. A similar version for the BATISS experiment would require an additional 2.5 thousand km of signal cable. Hence, a computer software program trigger selection is advocated for the large Issyk-Kul neutrino detector particularly for the cosmic-ray portion.

In conclusion, the minimum total length of all various types of cable required for BATISS will be on the order of 500 km.

13.6.3) The Electrical Power Requirements.

The source of the electrical power for the photomultiplier must provide a highly stabilized voltage. The voltages needed for the associated equipment are:

± 4.5 , ± 6 , ± 7.5 , ± 9 , ± 12 , ± 24 Volts.

About 2.3 kw of power are allocated for the high voltage for the photomultipliers. About 5 kw of power are allocated for the electronic modules. About 25 kw of power are allocated for the 36 minicomputers.

In such a manner a power supply (for an array located deep in water) must be able to deliver 32.5 kilowatts of power. The necessary power for the large land based computer will be about three kilowatts.

If we include various other sources of power demands associated with the BATISS experiment a total of 35 to 38 kilowatts of power is required to operate the experiment.

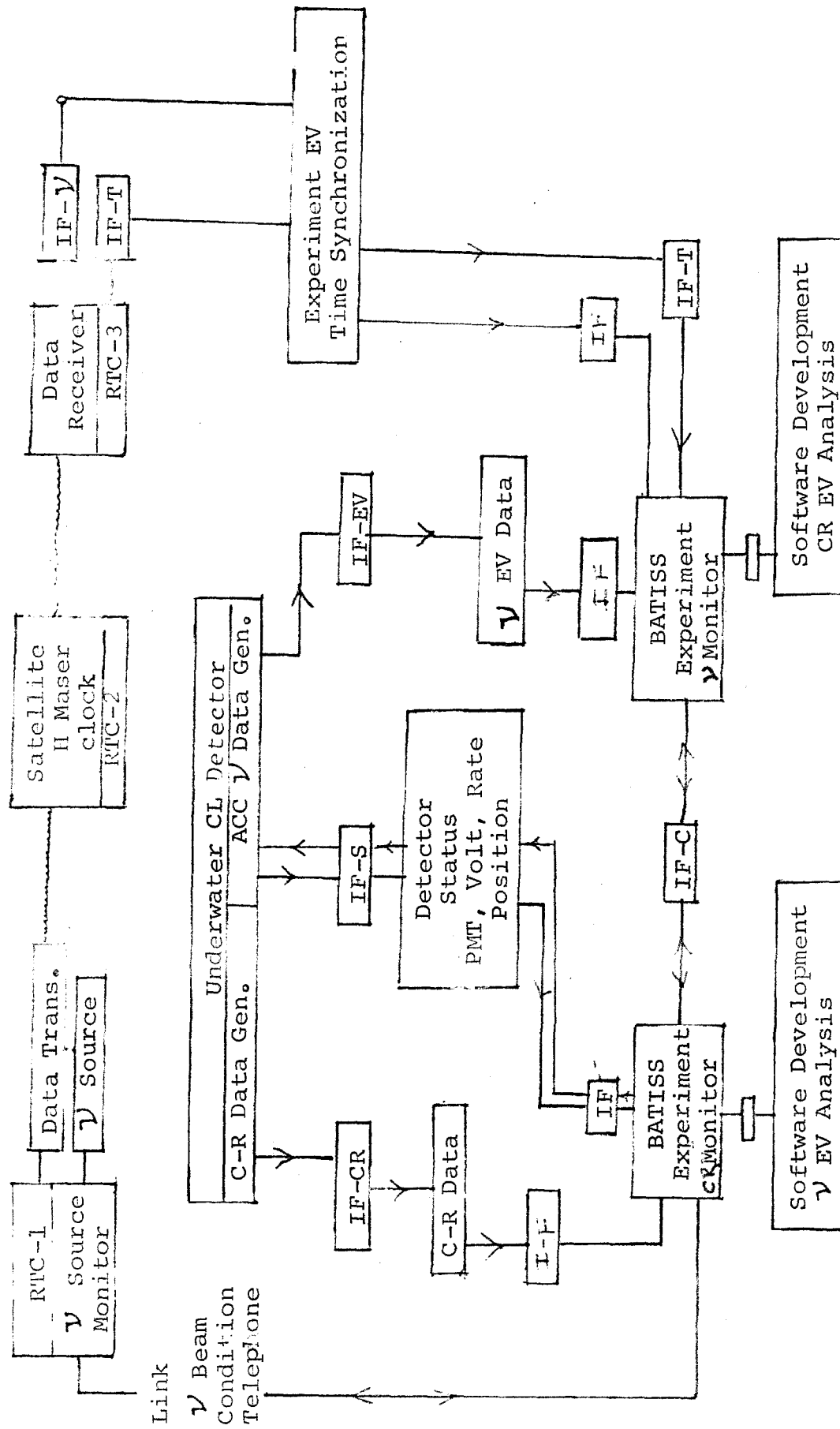
14.) Data Generation and Analysis.

14.1) Experiment Data Flow.

The organization of the data flow in the BATISS experiment is depicted in Figure 14.1-1. Two types of time synchronized data are required to be accumulated. First the conditions of the neutrino source and second, the detector response. The underwater Cherenkov light detector is depicted in the upper central portion of the Figure.

14.1.1) Neutrino Source.

The neutrino-source data acquisition system is shown in the upper left hand corner of Figure 14.1-1. At the time of each delivery of the neutrino beam information on the time of extraction of a particular bucket for each pulse must be recorded to at least one nanosecond of time jitter and to a comparable accuracy



BATISS GLOBAL DATA FLOW DIAGRAM

Figure 14.1.1-1

The meaning of the abbreviations are: RTC Real Time Clock, IF Data Interface Module, EV = Event, CR Cosmic Ray, CL = Cherenkov Light.

in the absolute time of extraction. It would be worthwhile to put this information on the Fermilab data logger for permanent storage.

Transmission of a Fermilab prepulse signal, prior to the fast NØ spill will allow the detector to be gated to record only those pmt pulses when the NØ neutrinos are passing through the detector. If a single turn extraction is used, an automatic reduction of noise by a factor of one million is possible.

It is also desired that the essential information for the extracted beam, its intensity and energy be transmitted in between deliveries from Fermilab.

Essential equipment should include a highly stable clock, a data recorder and a transmitter. A satellite is proposed to transfer time between the neutrino source and the detector and to serve as a data transfer point.

14.1.2) Neutrino Detector.

14.1.2-1) Cosmic-Ray Data.

The data flow from the detector is broken down into three components. The first is the flow of data from the upward looking portion dedicated to the study of high energy cosmic-ray muons and low energy (few GeV) solar flare neutrino interactions.

14.1.2-2) Accelerator-Neutrino Data.

The second data flow channel from the BATISS detector is from the downward looking portion dedicated to the detection of accelerator-neutrino events. In this case the trigger signal for the array can be very simple. A prepulse signal can be used to gate

the CAMAC data acquisition modules to accept only those (pulses from the photomultipliers) which occur during the passage of the neutrino beam. A master clock pulse giving the time of an epoch is fed into the modules of the array to be read by the array clock. The time of arrival of pmt pulses relative to the array clock is then recorded.

14.1.2-3) Array Monitor Data.

The third component of the data acquisition system of the array consists of data determining the status of each of the photomultiplier tubes and the relative position of the modules amongst each other. Control signals can be sent to the modules in the array to turn off defective tubes or to adjust the photomultiplier tube voltages to improve efficiency. Adjustments are needed to offset changes in tube efficiencies or signal transit times in the tubes.

Data from a separate module-position calibration system also flows along this path.

14.1.3) Data Network.

As indicated in Figure 14.1-1 the data flow amongst the various components of the experiment can take place with the aid of a network of minicomputers which interact with each other via telephone lines, satellite links and direct cables.

About 36 minicomputers will be required to carry out the detector data collection on a real time basis and three more for the monitoring of the neutrino sources, the time synchronization system and a reference telescope such as the one located at Western Washington University.

14.2) The Underwater Cherenkov Light Detector.

A methodology for the selection of data in BATISS is now discussed.

14.2.1) Accelerator-Neutrino Detector.

For the case of the Accelerator Neutrino Detector the data acquisition criteria are extremely simple. The array can be gated to accept only those events which occur during the expected time of passage of the neutrino beam from the accelerator. The FNAL regularly generates pulses of neutrinos 2 ms in duration for Bubble Chamber exposures. Since these occur in cycle times, T_{cy} , of around 10 second spacing, the background rejection is a factor of 5,000.

Single turn extraction of the Main Ring Beam takes $20\mu s$ and would have the advantage of a higher rejection in the background, on the order of 5×10^5 . In a $20 \mu s$ time period we expect to receive about 2 noise pulses per pmt on the average and occasionally a signal pulse. Hence, the timing prepulse from the accelerator could serve as the master trigger to initiate ADC of signals from every photomultiplier in that time period. On the average $756 \times 3 \times 2 = 4,536$ tube pulses are expected to be recovered from the array in the $20\mu s$ period.

The long time period between the accelerator-beam deliveries could then be used for a search and an analysis of recorded neutrino interactions.

14.2.2) Cosmic-Ray Detector.

The data acquisition procedure for the upward looking portion

of the array, consisting of 2,268 pmts housed in 756 modules is expected to be more sophisticated. It has to pick out high energy cosmic-ray muons and high energy muon interaction events. The master trigger must be provided from an internally generated fast trigger.

Such a trigger may be provided by an extremely bright pulse generated by the products of a high energy interaction or by a very high level of coincidence among the modules in the array corresponding to the traversal of a muon through the entire array. A muon must have a minimum of 36 GeV energy to overcome the ionization loss to get through the array.

From measurements of the underwater depth intensity distributions [36], [37] we estimate a rate:

$$I_{\mu} = 6.32 \times 10^{-5} \frac{\mu's}{cm^2-sec} \times 1.8 \times 1.8 \times 10^4 \times 10^4 = 20 \times 10^3 \mu's/sec.$$

with an energy greater than 36 GeV. Hence, in a day about 1.8×10^9 events could be recorded allowing for an extremely sensitive measure of the anisotropy of cosmic-rays.

14.3) Block Diagram of the Data Acquisition and Processing System.

The data acquisition and processing system for experiment BATISS is determined by the quality and amount of information necessary to achieve answers to the physics and geophysics questions stated in the preface. The system must be able to process and record the following information.

- 1) The absolute time of arrival of a pulse from a photomultiplier with an accuracy better than or equal to one nano-

second at the module and no more than 6 to 8 nano-seconds at the final destination where the information is recorded and analyzed by a number-crunching computer. The times of arrival of pulses relative to a neighborhood trigger pulse should be accurate to 50 ps.

2) The address of the module and the photomultiplier generating the pulse.

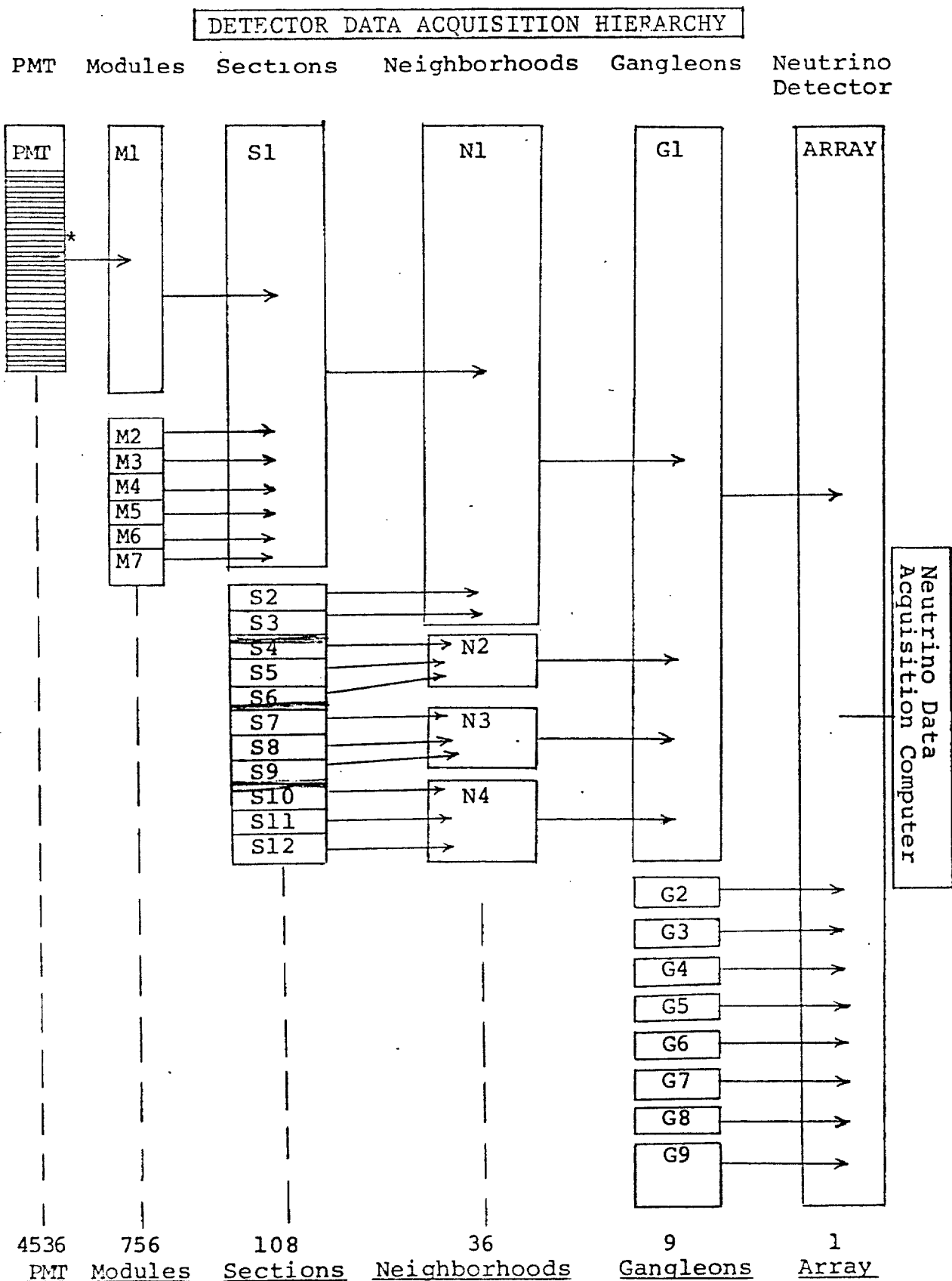
3) The amplitude of the signal pulse recorded at the module. The Cherenkov light intensities, A_{ijkn} , from a single particle ranges from one photoelectron from the most distant muon to about 300 for a muon passing through the center of the tube. That from an electromagnetic or hadronic shower is about 400 times greater.

The organization of the data acquisition system for the underwater neutrino detector is discussed in terms of a hierarchy of the grouping of the detector modules for the fourth variant of the detector array. These groupings begin with the two pair of three each of photomultipliers in a module, then groupings of 7 modules into a hexagonal section, then grouping of 3 sections into neighborhoods, then grouping of 4 neighborhoods into gangleons and finally the grouping of 9 gangleons into the detector array. The detector data acquisition hierarchy is shown in Figure 14.3.

14.3.1) Module Structure.

The basic module consists of 6 photomultiplier tubes (pmt's), three "looking up" (to observe cosmic-rays and their interactions) and three "looking down" (to observe accelerator neutrino

Figure 14.3



* An identical data acquisition hierarchy applies to the set of 756 x 3 downward looking photomultipliers.

events). The basic schematic of the electronics for one of the sets of pmt's within a module is shown in Figure 14.3.1 below. Its relation to other modules in the neighborhood of the array is shown in Figure 14.3.4.

14.3.2) Module Grouping and Address Structure.

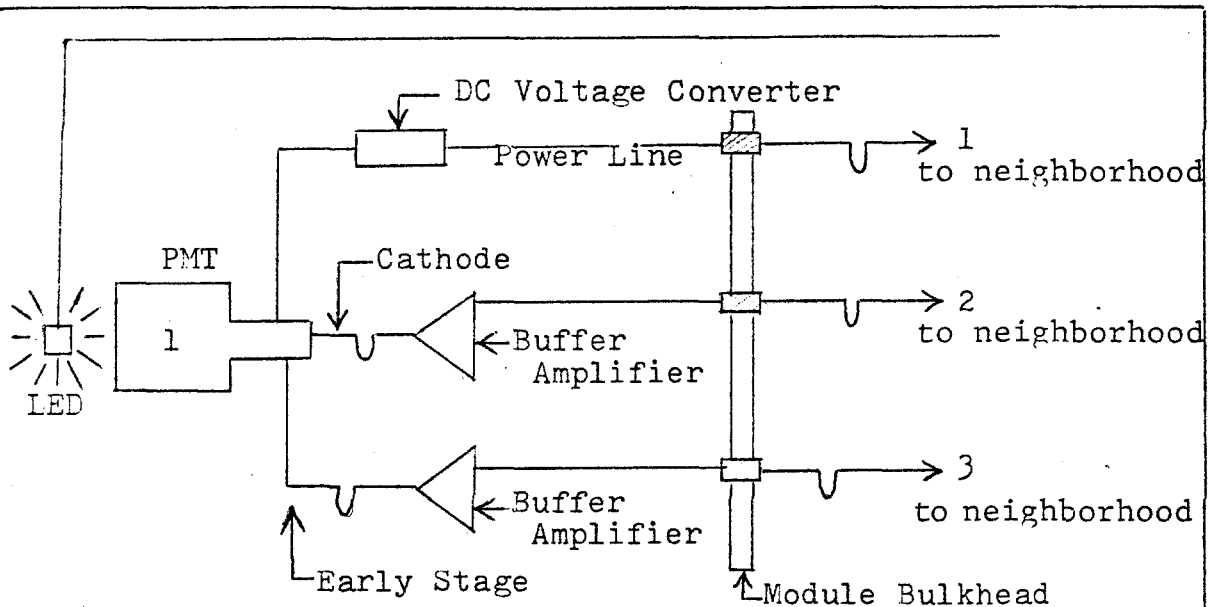
14.3.2-1) Address.

The photomultiplier tubes within each module are labeled $P_1 \dots P_6$ with $P_1 = u_1$, $P_2 = u_2$, $P_3 = u_3$. Here, u_1 , u_2 and u_3 label those looking up. The three downward looking portions can be labeled as $P_4 = d_1$, $P_5 = d_2$, $P_6 = d_3$.

The next grouping (Figure 14.3.2) consists of the set of seven modules, one at each of the six points of a hexagon and one in the center. The grouping considered as a unit is called a Section. Each module in the section is labeled as M_k with $k = 1 \dots 7$. Thus, each section consists of 21 photomultiplier tubes "looking up," and another 21 tubes "looking down." The address of each pmt is given by $M_k P_n$, $k = 1 \dots 7$, $n = 1 \dots 6$.

It is convenient to group twelve such sections into a unit, called a gangleon. The sections can be stacked so that the axis of the gangleon is parallel to the flight path of the accelerator neutrino. This configuration provides a high muon signal rate for modules along the string.

Continuing, it is natural to label the sections as $G_i S_j$ (where G_i labels the gangleon ($i = 1 \dots 9$) and S_j ($j = 1 \dots 12$) labels the section within the gangleon G_i). Nine such stacks can be grouped together to form a six million ton neutrino target-detector.



The rest of the 5 photomultiplier tubes and outputs are not shown.

- line (1) Low voltage dc power line to PMT High V. converter
- (2) Signal line for low amplitude Cherenkov light events.
- (3) Signal line for high amplitude Cherenkov light events.

<u>DC→DC</u>	Low to High Voltage Converters	— — — — —	6
<u>Photomultipliers</u>	RCA 4522	— — — — —	2
	FEY495	— — — — —	4
<u>Buffer Amplifiers</u>	— — — — —	— — — — —	12
<u>Penetrators</u>	50Ω	— — — — —	12
	High Voltage	— — — — —	6
<u>Housings</u>	— — — — —	— — — — —	6

Signal Cables to Neighborhood Intelligence Center:

12 signal lines each 240 meters long = 240 × 12 = 2880 m.
 high voltage lines each 240 meters long = 240 × 12 = 2880 m.
 490 m.

Figure 14.3.1 MODULE ELECTRONICS

One possible configuration using "off the shelf" hardware is shown above.

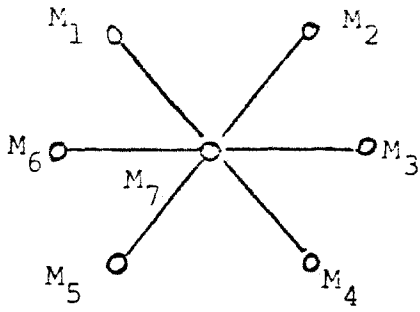


Figure 14.3.2
Labeling of modules in a
Section, S_4 .

Thus, the general address of each module will be labeled as $G_i S_j M_k$ and therefore, the complete address for each photomultiplier tube will be $A_{ijkl} = G_i S_j M_k P_l$ with ($i = 1 \dots 9$, $j = 1 \dots 12$, $k = 1 \dots 7$, $n = 1 \dots 6$).

14.3.3) Trigger Hierarchy.

Each physics experiment (accelerator-neutrino, cosmic-ray muon or proton decay) requires its own special trigger signature. Here we consider a "muon trigger" in detail which is used to signal an accelerator or cosmic-ray event.

For the purpose of defining a muon trigger, it is convenient to process data from a group of three adjacent sections. Let the set of three sections be called a neighborhood (see Figure 14.3-3). The overall electronics and their relation in a neighborhood is shown in Fig. 14.3.4.

We define a muon trigger whenever three or more modules within a neighborhood produce a signal within the transit time period of a relativistic particle passing through the neighborhood. This coincidence time period will be ≈ 90 ns. Since the two or three fold coincidence rate within a module will provide a cosmic-ray muon signal at a rate of about 15 per second the overall neighborhood trigger rate because of its larger area will yield a higher signal rate of about 105 μ 's per second. Pairs of muons with much less than the separation length between the modules can be detected by an examination of the signals from the sets of TDC's which are triggered by the event. Pairs as close as one foot can be separated from each other.

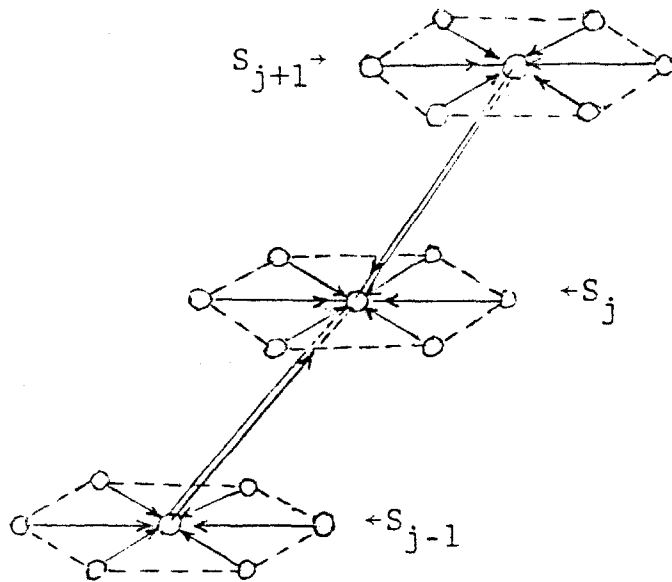


Figure 14.3.3

Neighborhood N_h .

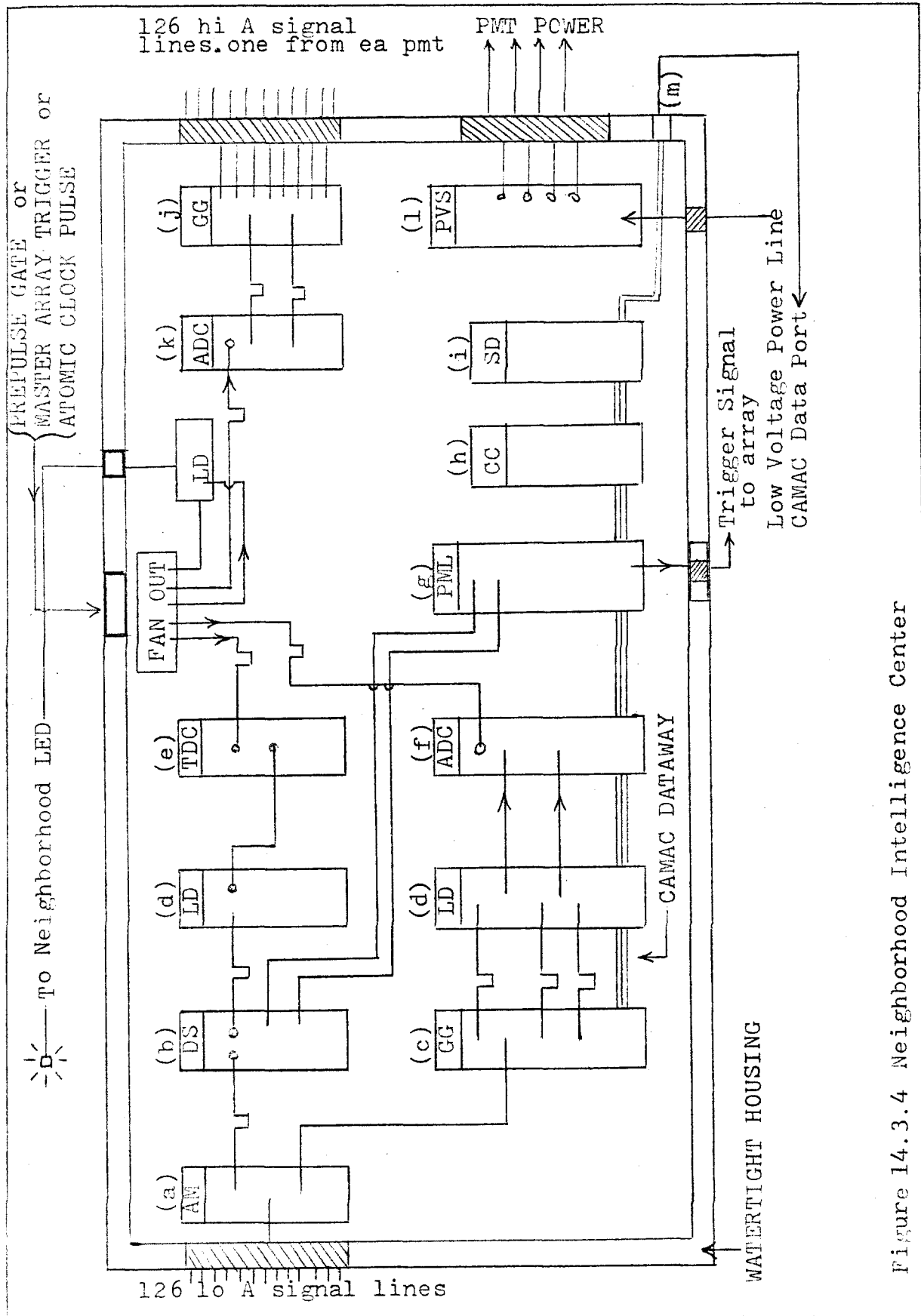


Figure 14.3.4 Neighborhood Intelligence Center

Figure 14.3.4. Neighborhood Intelligence Center

The Intelligence Center monitors and controls the high voltage supplies to the photomultipliers, provides electronics power, digitizes the time and amplitude of the PMT signals, tunes up the signal delays so that a precise programmable trigger signal can be generated and communicates with the array processor.

PART	#of channels	# of outputs/ channel
(a) AM Fast buffer amplifier	126	2
(b) DS Fast discriminator	126	2
(c) GG Gate generator	126	1
(d) LD Logic signal delay	252	2
(e) TDC Time to digital converter	126	-
(f) ADC Analogue to digital converter	126	-
(g) PML Programmable multi logic unit	126	1
(h) CC CAMAC crate controller	1	-
(i) SD Serial line Driver and converter to optical transmission	1	2
(j) GG Gate generator	126	
(k) ADC Analogue to digital converter	126	
(l) PVS Programmable DC Voltage supply	126	
(m) External data line		
(n) Full powered CAMAC crates		

14.3.3-1) Neighborhood

The parts for each neighborhood are listed below in Table 14.3.3-1.

Table 14.3.3-1

Parts List for One Neighborhood

1. Upward looking pmt's	21 x 3 = 63 pmt
2. Downward looking pmt's,	21 x 3 = 63 pmt
3. Number of modules,	7 x 3 = 21
4. Mixers	7 x 3 = 21
5. Cable Length(4 signal lines for each pmt)	$720 \times 0 = 10.8 \text{ km}$
6. Interfaces	21
7. Ribs	50

B. Power Cable. A three conductor power cable for each of the pmts is required. A total length of 3.15 km for one neighborhood is needed for this purpose also.

14.3.3-2) String Array.

One of the directions of symmetry of the array happens to be very close to the incident neutrino beam direction and hence the direction of the muons from the charged-current interaction. total of $9 \times 7 = 63$ strings of modules can be found which line up parallel to the axis of the neutrino beam in the full scale array.

A string, consists of 12 Cherenkov light detector modules along a line parallel to the line connecting the centers of the sections. The modules are spaced a distance of 15 meters, which is less than the absorption path of light in the water. This

configuration suggests a "hardware" technique for a signature due to "on-axis" muons. This is accomplished by adding a delay of $1/3\lambda_0$ to the signal cable of the module up stream relative to the immediate downstream module. Hence the signals from all of the modules along the string, due to a muon travelling upward at the speed of light along the axis of the string, will arrive simultaneously at the coincidence unit located at the top.

A trigger signal, generated when three or more coincidences occur from among the 36 photomultiplier tubes of a string within a time interval of 45 ns is required to start the TDC's clocks and ADC's charge integrating process. Later an examination of the photomultiplier data by an on-shore computer will use the pulses from each string to reconstruct the straight line trajectory corresponding to a particle traveling at the speed of light up through the string array. Data from one string will determine the direction of the muon to within the azimuth angle. By comparing data from two strings the trajectory will be determined to within two lines lying on the intersection of two cones and the data from the third string will produce the unique solution.

14.3.3-3 Gangleon.

Signals from the seven strings in one gangleon are controlled and processed by one minicomputer. A three-fold or higher majority logic coincidence from the outputs of any of the photomultipliers in a string can be used as a string trigger. The outputs of all 63 strings can then be sent through a mixer the output of which can be used as a gangleon trigger. This

gangleon trigger is used to digitize the information from all of the photomultipliers in the array.

This array trigger scheme requires the use of electronic logic delays of about $1.6\mu\text{s}$ for the outputs of all photomultiplier tubes before they are time digitized.

14.3.3-4 Transfer of Array Information.

After a master trigger is generated, the time of arrival, the amplitude, and the address of all of the signals generated within the array "looking time" interval are transferred to an on-shore mass storage device. This mass storage device then feeds the information to a number-crunching computer where software programs analyze the data.

14.4) The Detector Data Acquisition and Processing System.

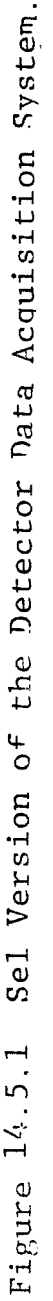
The data acquisition system consists of two main components, one designed to acquire and process the cosmic-rays which arrive at unpredictable times, and the second to acquire and process the accelerator neutrino events which arrive at predictable times.

It would be desirable to record the times of arrival and the amplitude of all of the signals above the one photoelectron level from each of the photomultiplier tubes in the neutrino detector array. Since the array consists of about $N = 5,000$ photomultiplier tubes, each of which produces pulses at the rate $R_1 = 10^4$ Hz, this would require that the data acquisition system have a signal data throughput capacity $C_1 = NR_1$, or 50 megahertz or 100 megabytes (for 16 bit data word lengths) per second.

The data acquisition system consists of two components. First, the set of all CAMAC modules which convert the $5 \times 10^3 \times 10^4$ pmt signals into computer compatible data and second, the set of minicomputers which multiplex the acquired data and feed it to a larger capacity computer for data processing.

By requiring a twofold coincidence between any pair of signals from the 21 modules in a neighborhood, the array trigger rate due to cosmic-ray muons is reduced to 4,000 events per second. The Cherenkov light from a single muon traversing the entire array will produce detectable signals in about 100 photomultipliers. Hence, a data acquisition system with a throughput rate of about 4×10^5 pmt signals per second is required. If each event must contain information about the amplitude and relative time of arrival and 2 byte words are required for both, then the cosmic-ray data throughput will be 1.6 megabytes per second.

One example of an adequate minicomputer system is the DEC VAX-11/780. This minicomputer has a 1.35 megabyte per second data transfer rate capacity and a four gigabyte virtual memory capability for operation of memory and software. An alternative data acquisition system utilizing the SEL 32/87 computer model 3820 is depicted in Figure 14.4-1. It has a 3.2 megabyte per second transfer rate.



14.4.1) Preliminary Processing:

The programs for the reconstruction of the event must give the trajectory of the muon (born in a charged - current neutrino interaction) and the development and the total energy from a hadronic cascade from the array data.

The basic array data consists of the set of amplitudes and the times of arrival of the Cherenkov light signals from a large number of modules. Preliminary processing by the underwater detector computers and onshore computers will select enriched neutrino interaction events. The event enrichment programs require that the onshore computer carries out a great number of elementary computations between beam spills. Some of these are:

1. Time Differences

Differences in the arrival time between signals or pulses from pairs of pmt tubes possessing a signal must be computed. Using the FNAL or BNL prepulse as a trigger the array can be gated open for a period of 20 μ s (FNAL) or a 3 μ s (for BNL). About two signal pulses per time gate are expected to be produced in each pmt in the 20 μ s spill and about 0.3 in a 3 μ s wide gate. A great many of the pulses will be noise signals which can be filtered out before permanent storage of the data.

The number of subtractions, N_s , which need to be carried out is:

$$N_s = \sum_{i,j=1}^{756} T_{ij} = \sum_{i,j=1}^N (t_i - t_j) = (756)^2 (3)^2 \approx 4 \times 10^6. \quad .14.4-1.$$

This operation must be carried out between the deliveries of the accelerator beams. In the case of the BNL this is 1.4 seconds and the FNAL about 15 seconds (for the tevatron it will be 60 seconds).

2. Speed of Light Data Cuts

A large number of logic operations must be carried out on the T_{ij} in order to filter out noise pulses. Each signal pair must satisfy the criterion:

$$T_{ij} \leq C_{ij} \quad \dots \dots \dots 14.4-2$$

where C_{ij} is the time it takes for a particle traveling at the speed of light to traverse the distance between a pair of modules i, j . In general, only about $7 \times 12 = 84$ modules (one ganglion) are expected to satisfy the criteria, but for exceptionally high energy interactions it is conceivable that signals from nearly all 756 modules will satisfy the criteria.

Hence, the number of logic operations, N_c , at this stage is expected to be about:

$$N_c = (756)^2 \approx 5.6 \times 10^5 \quad \dots \dots \dots 14.4-3$$

3. Straight Line Fits to the Muon Trajectory

The next set of operations is derived from the algorithms yielding trajectories of muons from the straight line fits to the TDC (time to digital converter) data. Trigonometric and other functions must be used to secure a best fit to the kinematic parameters of the event. Hence, it will be necessary to implement highly efficient software programs to hold down the number of computer operations to about 10^7 per event.

4. Detailed Analysis of Selected Events

About 120 accelerator neutrino events may be expected each day. The enrichment programs are expected to yield about 300 candidate neutrino events in a day. These will require longer event reconstruction programs taking about an order of magnitude longer period of time to process than the subtraction matrix or the Boolean operations of equation 14.5-2. A powerful on-site computer dedicated to the detailed analysis of the selected events could carry out the analysis in between spills. If the data are to be analyzed in between beam spill periods then it will be necessary for the selected computer to carry out about 10^7 arithmetic operations per second. No the countries possess such computers.

When the accelerator is not generating beam, the neutrino detector array can accept cosmic-ray neutrino data. About 300 cosmic-ray neutrino events may be expected each day. These may be used to extend the studies of atmospheric neutrinos carried out by the TKSAN neutrino detector.

15.) Budget Estimate.

15.1) Estimates of the Materials Cost of the Mechanical
Structure.

The basic structural elements are corrosion resistant duraluminum tubes each 15 meters long. About 6,000 structural members are needed for the array. Assuming a cost of \$3/meter the structural material will cost \$270,000.

About 756 module to array interface structures are also needed. At \$30 an interface we estimate a cost of \$22,680. In addition, welding supplies, bolts and anti-corrosion elements are

also needed. These supplies should total about \$25/module which amounts to a total cost of \$18,900 for miscellaneous materials.

In summary the material costs for the structure are:

1) 6,000 structural members each 15 meters long	\$270,000
2) 756 module to array interface structures	22,680
3) anticorrosion metals, bolts, welding supplies	<u>18,900</u>
	\$311,580

15.2) Estimates of the Cost of the Electronics in the Data Acquisition System.

These estimates are made for an array consisting of 756 modules. Each module consists of six photomultipliers, three looking up and three looking down. The data acquisition system determines the time of arrival of a Cherenkov light pulse, the amplitude and the address of the photomultiplier. The total cost is estimated to be \$11,650,000 for a specific system using off-the-shelf hardware as listed in the table below. Costs are in 1981 dollars.

1) Amplifiers LeCroy 612A 12 Channels with x 10 amplification.

756 modules x \$1295/unit (108 sections)	\$979,020
--	-----------

2) Analogue to Digital Converters.

LeCroy 2282 48 channel 1 ns resolution	217,350
--	---------

LeCroy Systems Processors, 4 units @ \$1,500	10,000
--	--------

3) Time to Digital Converter. 1 ns resolution

LeCroy 4291B 32 channel drift chamber TDC

$\left(\frac{\$3,000}{\text{unit}} \right) \frac{(4536 \text{ pmt channels})}{(32 \text{ channels/unit})} = \$3,000 \times 142$	425,250
--	---------

4) Coincidence Units.

LeCroy 380A: 108 sections x 2 units/section	236,520
Alternate: 216 sections x \$1095	
6,912 channels 756 up	(25,869)
2,268 channels 756 down	(25,869)

5) Discriminators.

LeCroy #825	
Quint risetime disc \$1450 x 756 modules	1,096,200
Alternates: model 77705 32 channel (\$700)	
142 units + 14 = 156 at \$710	(110,760)

6) High Voltage Supplies.

HV4032A 32 negative outputs @ \$5,700	873,600
Alternate: \$80/channel for Venus x 4536	(362,880)

7) Cables.

500 km @ \$ 3,000/km	1,500,000
Total for ADC, TDC, Power, cables.	
Multiconductor cable	

8) Photomultiplier Tubes.

RCA 4522: 756 x 6 = 4,536 x \$800	3,628,800
FEY 49: 5,000 @ \$200	1,000,000

9) Mini Computers.

KS 8030 @ \$12,000 x 10 units	120,000
Alternate: DEC PDP11 @ \$20,000 x 10 units	(200,000)

10) Time Synchronization System.

5 Hydrogen Maser Clocks @ \$300,000	1,500,000
-------------------------------------	-----------

Total Electronic Equipment Costs	\$11,650,000
Cost Using Alternate Equipment	(\$6,356,998)

15.3) Costs of Electronics for the Hexagonal Sections.

This electronics will assemble and sort signal pulses prior to recording by the array computer system. Below is a detailed list needed for two sections. The total cost for the complete array is given in section 15.2

	<u>Description</u>	<u>Price</u>	<u>#Units</u>	<u>Total</u>
1.	TD811 8 channel each (E.G.G. CAMAC Time Digitizers	\$1,400	11	\$15,400
2.	2259A 8 channel each (Le Croy CAMAC Analog Converters)	1,400	11	15,400
3.	RC014 (E.G.G. CAMAC Real Time Clock) - Interface between array and atomic clock	1,500	1	1,500
4.	LG105/NL (E.G.G. Linear Gate/Stretchers)	1,000	81	81,0
5.	81-input coincidence units with presettable plurality selection (Custom)	2,000	1	2,00
6.	621BL (Le Croy Quad Discriminator) 4 discriminators/Unit	1,195	1	1,195
7.	1 - 11 Fanout (Custom)	1,000	2	2,000
8.	1 - 81 Fanout (Custom)	2,000	1	2,000
9.	Model 2000 Canberra NIMBIN	738	10	7,380
10.	Environmental Protection for above (Circuit Board Coating)			1,000
11.	CAMAC Circuit to sense ambient light levels	1,200	1	1,200
12.	Total			\$130,075

15.4.) Cost of On-Shore Data Processing Systems.

The following is an estimate of the cost of the on-shore data processing systems using the Digital Equipment Corporation VAX 11 computer as an example. The SEL may be better and less expensive.

I. VAX 11/780 Package.

This is to be used at the detector site

for data acquisition and processing.
Fully configured 13 Mbytes, 256 Mbytes
disk, tape drive 125"/sec.

257,000

II. VAX 11/750 Package.

To be used at WWU for accelerator
neutrino data analysis. CPU BUSS
capacity of 13.3 mbytes/sec.

- 1) 11/750 up with 512 Kbytes of MOS.
- 2) LA38 Decwriter console 24 Kbytes.
- 3) RK078-11 Controller and drive. Two
RK07 disks each 28 Mbytes of storage.
- 4) QD001-AD VAX/VMS operating system.
- 5) Unibuss Adapter
- 6) Subtotal

89,900

Peripherals.

- 1) TU58-N tape cartridge drive. 2,048
records x 128 bytes 1,500
- 2) VT100-AA video terminal 2,150

Mass Storage Devices.

- 3) RM05-BC (256 Mbytes) 39,140
- 4) TEU77-CB master tape, 200 Kbytes/sec
40 Mbytes/reel 35,000
- 5) TU77-AF slave tape 23,000
- 6) LA120 terminal 2,950
- 7) Subtotal 103,740

IV. Maintenance Contract.

12 Mo. @ \$710/Mo.

8,5

V. CPU Options.

1) 2nd memory controller for 11/780, 74 Megabytes, 4096 Kbytes	26,600	
2) 7 units of 256 Kbytes of mass memory each \$9,100	63,700	
3) FPA floating point accelerator for 11/780 Requires 0.8 μ 's for a + or - and 1 μ 's/ degree of polynomial.	10,000	
4) Multiport memory option	37,300	
5) 7 units of 256 Kbytes of mass memory each \$9100	63,700	
6) User control store 12 Kbytes	10,700	
7) Battery backup pack	1,250	
8) Cabinets	17,840	
9) Subtotal		231,090

VI. Input-Output.

1) DMR 11-AA interface serial line interface	4,200	
2) MA780-AA mass buss adapter 32 byte with silo data buffer	37,300	
3) LPA11-K front and back	5,000	
4) Three modems Bell Telephone module 208 @ \$400 each	1,200	
5) Unibuss adapter (18 bit) - DZ11-E 15 NPR with a 4-16 bit buffer @ 1.35 Mbytes/sec.	4,300	

6)	2 Com Data model 370E2-42 Phonem @ 337. WWU, FNAL	774	
7)	TI 765 Terminal - modem	3,029	
8)	Subtotal		55,803
VII. <u>Software.</u>			
1)	DECNET	3,100	
2)	MUX200/VAX Multi-terminal emulator QE070-AY for Cyber series CDC 6600 with IBM Standard Protocol for 200 UT Mode 4A communications channels	8,100	
3)	VAX11-3271 Protocol emulator for the 11/780 processor	7,500	
4)	VAX11-2780/3780 Protocol emulator for IBM Standard protocol	5,900	
5)	FORTTRAN Compiler	8,050	
6)	VAX 11 DSM data management system	12,000	
7)	Engineering Graphics Utilities	2,500	
8)	Subtotal		47,150
VIII. <u>Array Processor.</u>			
	Floating Point Systems	55,000	
	Unibuss 100' Ribbon Cable BC11-A5	644	
	Unibuss Repeater (One for each 50 feet)		
	Coaxial Cable 1000'	680	
	Subtotal		4,424
IX. <u>Documentation.</u>			
1)	VAX-11/780 Hardware Documentation	100	
2)	Maintenance Documentation Service	4,800	

3) Source Listings	25,000	
4) FORTRAN, Documentation	78	
5) Subtotal		<u>29,978</u>

X. Supplies

1) Disk packs RK07K-DC @ \$430 x 10	4,300	
2) Disk packs PR05-P @ \$1,450 x 4	5,800	
3) Magnetic tape, 9-track, 100 tapes @ \$30 ea	3,000	
4) Cables	5,000	
5) Busses	5,000	
6) Subtotal		<u>23,100</u>

XI. TOTAL		<u>\$896,465</u>
-----------	--	------------------

XII. SUMMARY OF EQUIPMENT COSTS

1) Structural	\$ 311,580	\$	
2) Electronics	10,586,740		
3) Computer	896,465		
TOTAL			<u>11,794,785</u>

Total Administrative and Salary	10,000,000	
Bending of the FNAL Neutrino Beam	40,000,000	
Total Project Cost		<u>\$61,794,785</u>

16.) List of References.

1. E. V. Kolomeets, V. S. Murzin, L. I. Sarecheva, S. A. Askarova, "Experiment 'BATISS' Neutrino Illumination of the Earth" Publisher KITAP Alma-Ata 1979.
2. E. V. Kolomeets, V. S. Murzin, Geophysical Journal (West Germany) 1980 - In press.
3. D. Sh. Eleukenov, K. G. Karsakpaev, E. V. Kolomeets, Iu. V. Katlov, V. C. Murzin, Iu. B. Prelepsy, G. A. Elkin, "Proceedings of the International Seminar on Cosmophysical Aspects in the Study of Cosmic-Rays" page 95 Published by KITAP Alma-Ata 1980.
4. E. V. Kolomeets, V. L. Schmonin, 14th ICCR, 2c Munchen 1975.
5. J. A. Albers, R. Davisson, S. Kondratich, P. Kotzer, R. Lindsay, R. Lord, S. Neddermeyer, Proceedings of the XVI ICCR, Kyoto, Japan, 1979.
6. R. Bostrom, P. Kotzer, Bulletin of the American Physical Society, January 1979.
7. E. V. Kolomeets, JETP 36 5 1351 (1959).
8. E. V. Kolomeets, Proceedings of the International Seminar in Leningrad 205, Leningrad (1973).
9. S. M. Schindler, P. D. Kearney, Nature 237, 503 (1972).
10. S. M. Rilendy and B. M. Pontecorvo, Usp. Fizi. Nauk 123, 2, 161 (1977).
11. S. G. Petkov, Nuclear Physics 25 641 (1977).
12. V. A. Lybimov, E. G. Novikoff, V. Z. Nosik, E. D. Tretyakov, V. S. Kozik, Physics Letters 94B p 266 (1980).

13. T. Eichten et al. Physics Letters B46, 277, 281 (A73).
14. P. F. Ermolov, A. I. Muhin, Usp. Fiz. Nauk Vol. 124, 1978.
15. R. Davis, Jr., John Evans, Proceedings of the VI Leningrad International Seminar 91, (1974).
16. N. Erlov "Optical Oceanography" Published Mir 1970.
17. V. V. Shulakin "The Physical Sea" Fourth Edition 1968, USSR-AS.
18. R. Ivanov, Journal of Geophysics VIV part 2-3, 1936.
19. V. S. Murzin "Introduction to the Physics of Cosmic-Rays" Moscow, Atomzdat, 1979.
20. J. Albers, P. Kotzer, "Wide Angle Neutrino Fluxes and Heavy Neutrino Mass Limits" WWU (1980).
21. D. B. Cline, Experiment to Detect Proton Decay and Neutrino Oscillations, Preprint C00-088-180, Univ. of Wisconsin.
22. J. J. Simpson, Phys. Rev. D, 23, 649 (1981).
23. see R18
24. T. Kondo, Bull. Am. Phys. Soc., 26, 38 (1981).
25. Malensek et al. Private Comm. with Fermilab (1979).
26. Fermilab Report 1979. Neutrino Group.
27. S. Anderson and J. Lord, "Radioactivity of Sea Water" in "Proceedings of 1975 Summer Workshop on Neutrino Interactions in the Ocean Depths and on Oceanographic Physics and on Marine Engineering," ed. P. Kotzer, Western Washington University, 1976.
28. H. Primakoff, "Proceedings of Neutrino 78", Earle C. Fowler, Editor.
29. V. Barger, K. Whisnant and R. J. N. Phillips, Phys. Rev. Letts., 45, 2084 (1980).

30. E. W. Kolb and T. J. Goldman, Phys. Rev. Letts., 43, 897 (1979).
31. C. Albright, "Proceedings of the International Conference on Neutrino Physics and Astrophysics: Neutrino 79," Bergen, Norway (1979).
32. F. Reines, H. S. Gurr and W. Sobel, "Proceedings of the International Conference on Neutrino Physics and Astrophysics: Neutrino 80," Erice, Italy (1980).
33. J. Learned, F. Reines and A. Soni, Phys. Rev. Lett., 43, 907 (1979).
34. C. O. Alley, LASSO A Proposal for Satellite Time Transfer.
35. M. M. Boliev, et al., "Proceedings of the XVIIth International Cosmic-Ray Conference," Paris, Vol. 7 (106) 1981.
36. V. M. Fyodorov and Yu. A. Trubkin et al., "Depth Intensity of Cosmic Ray Muons to 3,000 Meters of Water," Bulletin of the Academy of Sciences of the USSR, 34, 1759 (1970).
37. Higaski et al., II Nuovo Cimento 433, 334 (1966).

- 38. P. Nemethy et al., Phys. Rev. D 23, 262 (1981).
- 39. F. Boehm et al., Phys. Rev. Let. 97B, 310 (1980).
- 41. R. N. Mohapatra, G. Senjanovic, "Neutrino Masses and Mixings in Gauge Models with Spontaneous Parity Violation", Phys. Rev. D 23, 165 (1981).
- 42. M. Krishnaswamy, M. Menon, N. Mondal, V. Naraslimham, B. Sreekantan, N. Ito, S. Kawakami, Y. Hayashi and S. Miyake, Phys. Let. 106B (1981) 339.
- 43. J. Albers, B. Faber, E.V. Kolomeets, P. Kotzer, R. Lindsay, R. Lord, V.S. Murzin, S.H. Neddermeyer, A. Rupaal, C.S. Schmidling, R. Webster, "Search for Neutrino Like Events 2,750 km from the Source," Proceedings of the 18th ICRC Bangalore India (1983). (to be published).

17.) Acknowledgments.

The authors wish to express their appreciation to Vladimir Milicic and Beth Jacobson for their assistance in translating portions of this publication from the Russian.

To Jere J. Lord for valuable discussions regarding neutrino interactions, hadronic and electromagnetic cascades.

To Larry Steele Company for the survey of the BATISS Telescope at Western Washington University.

To Dorothea Kotzer, Ellen Evans, Christopher Kotzer, and Georgia Popple for preparation of this manuscript and for many of the drawings.

To Jim Webster for preparation of the photographs.